frontiers in Pharmacology

REVIEW
published: 11 December 2020
doi: 10.3389/fphar.2020.579332

Hydroxysafflor Yellow A: A Systematical Review on Botanical Resources, Physicochemical Properties, Drug Delivery System, Pharmacokinetics, and Pharmacological Effects

Feng Zhao[1†], *Ping Wang*[1†], *Yuanyuan Jiao*[2], *Xiaoxiao Zhang*[3,4,5], *Daquan Chen*[6] *and Haiyu Xu*[1,7*]

[1]Institute of Chinese Materia Medica, China Academy of Chinese Medical Sciences, Beijing, China, [2]Tianjin University of Traditional Chinese Medicine, Tianjin, China, [3]Resource Center for Chinese Materia Medica, China Academy of Chinese Medical Sciences, Beijing, China, [4]Postdoctoral Management Office, China Academy of Chinese Medical Sciences, Beijing, China, [5]China Association of Chinese Medicine, Beijing, China, [6]School of Pharmacy, Yantai University, Yantai, China, [7]Shaanxi Institute of International Trade and Commerce, Xianyang, China

Hydroxysafflower yellow A (HSYA), as a principal natural ingredient extracted from safflower (*Carthamus tinctorius* L.), has significant pharmacological activities, such as antioxidant, anti-inflammatory, anticoagulant, and anticancer effects. However, chemical instability and low bioavailability have been severely hampering the clinical applications of HSYA during the treatment of cardiovascular and cerebrovascular disease. Therefore, this present review systematically summarized the materials about HSYA, including acquisition methods, extraction and detection methods, pharmacokinetics, pharmacological effects and molecular mechanism, especially focus on the possible causes and resolutions about the chemical instability and low bioavailability of HSYA, in order to provide relatively comprehensive basic data for the related research of HSYA.

Keywords: hydroxysafflor yellow A, bioavailability, biological activity, chemical stability, delivery systems, botanical resources

OPEN ACCESS

Edited by:
Yanqiong Zhang,
Institute of Chinese Materia Medica, China

Reviewed by:
Guibo Sun,
Chinese Academy of Medical Sciences and Peking Union Medical College, China
Tan Loh Teng Hern,
Guangdong University of Technology, China
Shuzhen Guo,
Beijing University of Chinese Medicine, China

***Correspondence:**
Haiyu Xu
hyxu@icmm.ac.cn

[†]*These authors have contributed equally to this work*

Specialty section:
This article was submitted to Ethnopharmacology, a section of the journal Frontiers in Pharmacology

Received: *02 July 2020*
Accepted: *23 October 2020*
Published: *11 December 2020*

Citation:
Zhao F, Wang P, Jiao Y, Zhang X, Chen D and Xu H (2020) Hydroxysafflor Yellow A: A Systematical Review on Botanical Resources, Physicochemical Properties, Drug Delivery System, Pharmacokinetics, and Pharmacological Effects. Front. Pharmacol. 11:579332. doi: 10.3389/fphar.2020.579332

INTRODUCTION

Cardiovascular and cerebrovascular disease (CCD), as one of the leading causes of mortality worldwide, has been increased rapidly and presented younger trend, with high mortality all of the world (Collins et al., 2017; Donahue and Hendrikse, 2017). Although many types of therapeutic strategies were used to treat patients with CCD, such as angiotensin converting enzyme inhibitor (ACEI), ß-receptor blocker, and statins, the outcome remains not satisfactory due to the inevitable side effects and high treatment expenditure. To address the problem, more and more studies are trying to seek treatment strategy from Traditional Chinese Medicine (TCM). Characterized by minor side effects, TCM has become an important source of natural product, such as Aspirin, Digoxin, Hydroxysafflor yellow A, which exhibit substantially protective effects against CCD (Eichhorn and Gheorghiade, 2002; Dai and Ge, 2012; Desborough and Keeling 2017; Hu et al., 2020).

Hydroxysafflor yellow A (HSYA) is a primary active product derived from safflower (*Carthamus tinctorius* L.), a plant of the *Compositae* (*Asteraceae*) family, which was used to improve blood circulation, eliminate blood stasis, and relieve menstrual pain as early as recorded in *Kaibao Bencao*. HSYA, as an indicator component to characterize the medical value of safflower recorded in *The Pharmacopoeia of the People's Republic of China* from 2005 edition, possesses a broad spectrum of pharmacological activities, such as antioxidant, anti-inflammatory and anticoagulant effects, which play an important role acting on cardiovascular and cerebrovascular disease (Sun et al., 2010; Wu et al., 2012; Ma et al., 2019a; Zhou et al., 2019; Bacchetti et al., 2020). However, chemical instability and low bioavailability of HSYA severely hamper the clinical applications. It can be easily oxidized, hydrolyzed, polymerized by light, high temperature, and alkaline conditions due to its structural characteristics. The high polarity directly leads to difficulty of transmembrane transport, resulting in low bioavailability. To address these problems, new drug delivery systems were developed to improve the therapeutic efficacies of HSYA based on lipid-based carriers, such as microemulsions, self-emulsifying systems, nanoparticles, chitosan, and the combination of HSYA with other drugs, which may have a good application prospect.

The present review systematically summarized the literatures about HSYA, including botanical resources, extraction and detection methods, pharmacokinetics, pharmacological effects and molecular mechanism, especially focus on the possible causes and resolutions about the chemical instability and low bioavailability of HSYA, in order to provide relatively comprehensive basic data for the related research of HSYA.

ACQUISITION OF HYDROXYSAFFLOWER YELLOW A

HSYA is mainly extracted from safflower, but the amount is not enough to support current clinical applications. Therefore, it is urgent find other ways to obtain HSYA. At present, chemical synthesis and biosynthesis are two promising ways to obtain HSYA. The information was detailed as follows.

Acquisition From Safflower

Safflower, as the natural source of HSYA, is widely planted worldwide. It is said that safflower originated in West Asia (Iran, Nicaragua and Turkey), and were later introduced for cultivation on almost every continent except Antarctica, such as America, Australia, China, Ethiopia, India, Italy, Mexico, Spain, and so on (**Figure 1**). India has developed into the most productive country with the planting areas of over 760,000 hm^2, and the yield of about 460,000 t, accounting for 50% of the total area and yield in the world (Liang et al., 2015).

Safflower is also widely cultivated in China with planting area of about 30,000–58,000 hm^2, and dried flowers yield of about 1,500–2000 t every year. Xinjiang province has become the major safflower production area, covering an area of 16,700–40,000 hm^2, which accounts for more than 3/4 of the total planting areas and provides more than 80% dried flowers and seeds in China. Henan province (*Weihonghua*, 卫红花), Zhejiang province (*Duhonghua*, 杜红花) and Sichuan province (*Chuanhonghua*, 川红花) are described as the authentic product areas of safflower in the history of China.

The content of HSYA containing in safflower were affected by many factors, including geographical origins, color and harvest time. The content of HSYA ranged from 0.05 to 14.99 mg/g by comparing 80 safflower cultivars collected from Africa, America, Asia, and Europe. HSYA in Africa cultivars was higher than that in Asia and Europe, and China cultivars is higher than that in Turkey, India and Kenya. Moreover, color is another factor to influence the content of HSYA. The darker the color of safflower, the higher the content of HSYA (red > orange > yellow > white according to PANEONE) (Tong et al., 2011; Xu et al., 2018). For example, Hebei safflower (red) was richer in HSYA (26.943 mg/g) than that in Wei safflower (white flowers, 0.472 mg/g) in China (Zhao, 2015). The most appropriate time to pick safflower is the

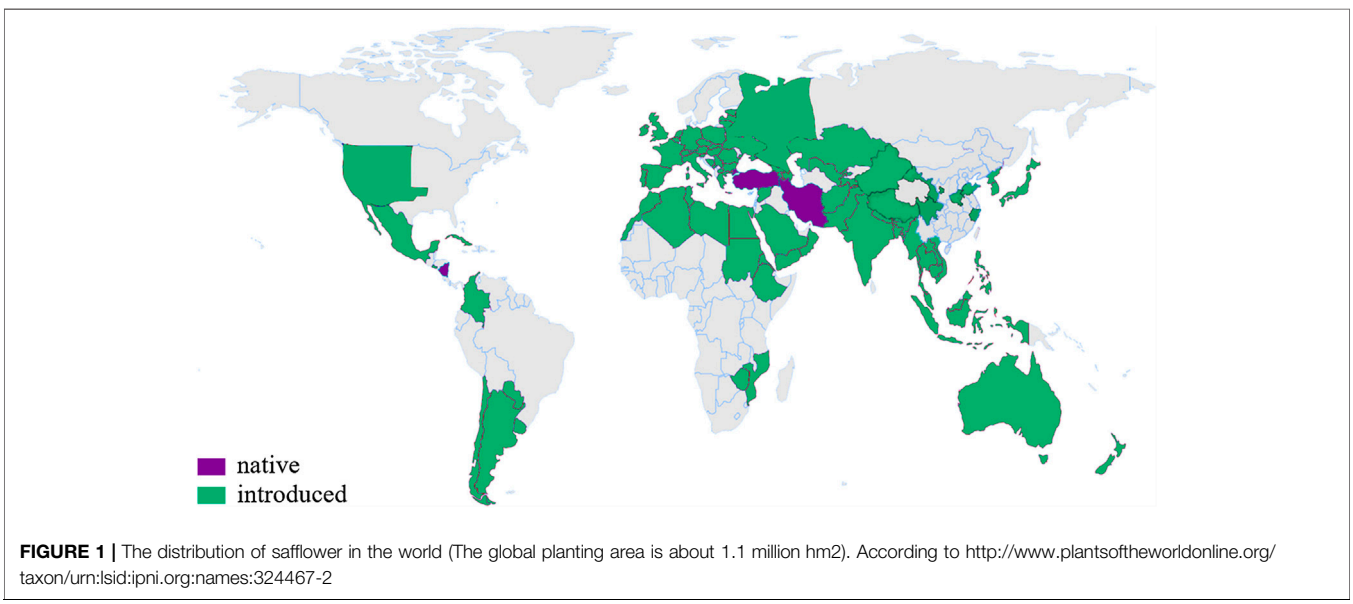

FIGURE 1 | The distribution of safflower in the world (The global planting area is about 1.1 million hm2). According to http://www.plantsoftheworldonline.org/taxon/urn:lsid:ipni.org:names:324467-2

morning of the third or fourth day after flowering (Tian et al., 2007).

Oxidation Synthesis Pathway

Chemical synthesis is an efficient way to obtain the natural or unnatural products within a short time period. Oxidation synthesis for HSYA is a rapid and highly efficient chemical synthesis method, and the synthetic pathway was shown in **Figure 2A**.

According to a retrosynthetic analysis of HSYA, di-C-glucosyl chloroacetophenone (3) transformed into di-C-(per-O-acetylglucosyl) phloroacetophenone (4) with BF_3.2AcOH at room temperature for 5 h. A further oxidation afforded the phenolic hydroxyl-free glycoside (5) with the quinol. Moreover, the two enantiomers of 4-(S)-2-acetyl- 4,5-dihydroxy-4,6-di-C-β-D-glucosyl-3-methoxycyclohexa-2,5-dienone (6) was obtained after diazomethane added to acetic acid solution of product 4 at 0°C. Finally, compound 6 transformed into HSYA (7). Compared the oxidant synthesis pathway mentioned above, di-C-glucosyl chloroacetophenoneoxidation (1) was converted into di-C-glycosylquinol(2) via an oxidation, and then was directly transformed into HSYA (7) with the yield at 18%, suggesting it is worthy promoting in the future (Suzuki et al., 2017).

Biosynthetic Pathway

Biosynthesis is a multi-step enzymatic process, in which a simple product is converted into a more complex desired product in a living organism. Biosynthesis is characterized by continuous and effective production, low-carbon and friendly environment, which provides a great support to the development of natural products (Pang et al., 2015). This production model will be the main source of HSYA in the future. However, the biosynthetic pathway of HSYA in plant remains unclear. According to the vital reaction of chalcone biosynthetic pathway, one molecular of 4-coumaroyl-CoA and three molecules of malonyl-CoA are converted into naringenin chalcone (4,2′,4′,6′-tetrahydroxychalcone) via the intervention of chalcone synthase, and it was transformed into HSYA after glycosylated (Heller and Hahlbrock, 1980; Knogge et al., 1986). The possible biosynthetic pathway of HSYA in phytosomal was shown in **Figure 2B**.

The content of HSYA is controlled by a nuclear gene with two alleles, HSya and hsya gene. HSya gene dominates completely over hsya gene to promote HSYA biosynthesis (Zhang et al., 2009; Yang et al., 2011). *sHSP* is a small heat shock protein and encoded by CTL-*hsyapr,* which might be directly or indirectly disturb HSYA biosynthetic pathway (Tang et al., 2010). When safflower is under external pressure, CT-*wpr* (TDF-11) was activated, which might arouse *sHSP* and inhibit the expression of HSya to some extent, finally leading to the inhibition of biosynthetic pathway of HSYA (Li et al., 2010b).

EXTRACTION AND DETECTION

Extraction Methods

HSYA is highly soluble in water, while hardly dissolve in lipophilic solvents such as ethyl-acetate, ether, benzene, and

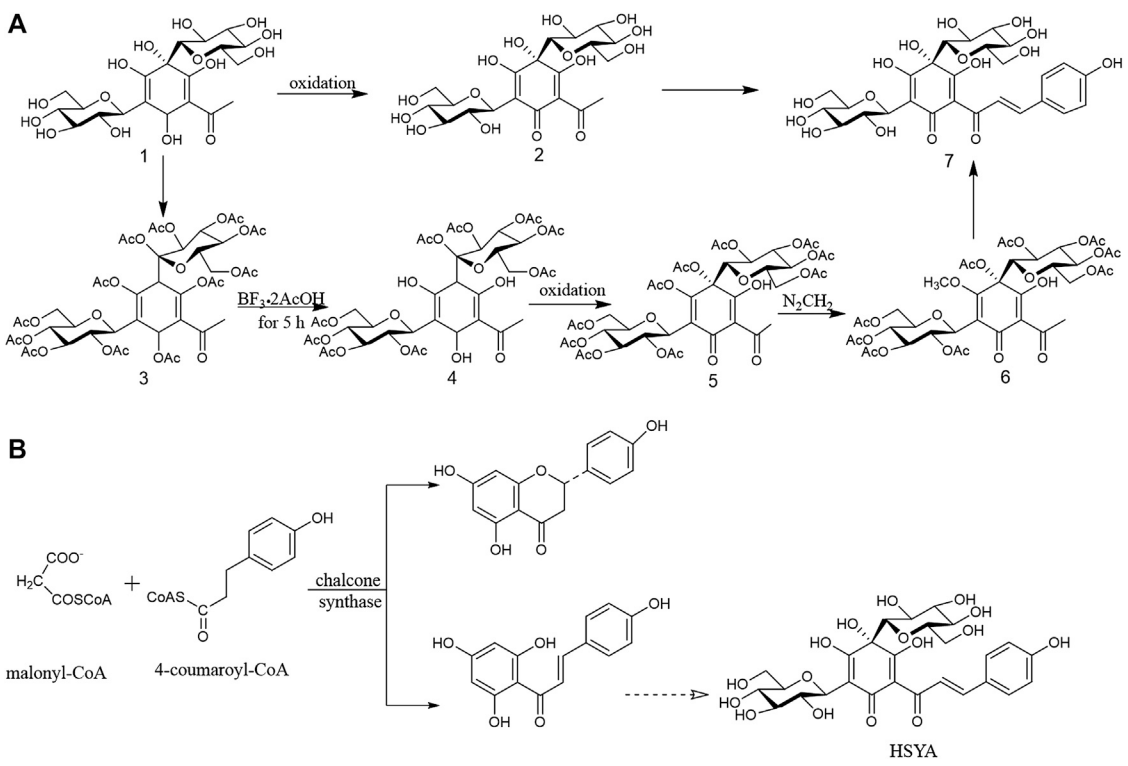

FIGURE 2 | (A) Oxidative synthesis pathway of HSYA; **(B)** The possible biosynthetic pathway of HSYA in phytosomal.

TABLE 1 | Representative examples of the extraction and purification methods of HSYA.

No	Total sample	Method	Pre-treatment	Extraction	Purification	Yield	Additional notes	Referencces
1	800 g	Water immersion	NA	Distilled water (10 L, 80°C, 20 min) for 2 cycles	The extracts were combined, evaporated and filtered	0.023%	NA	Li et al. (2013)
2	2000 g	Water immersion	The fresh flowers were shade dried and powdered	Distilled water (60°C, 30 min, 20 L) for three times	The solvent by evaporation under the reduced pressure, the residue was dissolved in 10% ethanol (1,000 ml), then evaporated to dryness under vacuum to afford a residue	0.066%	NA	Bai et al. (2012)
3	1 g	MAS-I microwave extraction system	NA	Distilled water at 70 °C for 20 min with solid and liquid ratio 100 for 3 cycles, and then the extracts were filtered	NA	6.96%	NA	Yang et al. (2008)
4	0.5 g	UAE extraction system	NA	Ultra-pure water (55°C, 39 min, liquid-to-solid ratio of 16) in ultrasonic (40 kHz, 250 W) for 3 times	The extracts were filtered, and transferred to 100 ml volumetric flask, filtered by a 0.22 μm filter	1.798%	Reflow by cold water during ultrasonic procedure	Sun et al. (2013)
5	20 g	Smashing tissue extraction system	NA	Distilled water with liquid-to-solid ratio of 40, at 2.5 min for 90 V, and filtered	NA	1.359%	NA	Wang et al. (2012)
6	500 g	Alcohol extraction method	NA	75% aqueous ethanol (3,000 ml, 12 h) for 10 cycles	The extracts were concentrated to dryness in *vacuo* at 55°C, re-solved with water, and extracted by petroleum ether and ethyl acetate for five times	0.584%	RP-MPLC was used to isolate and purify	Zong et al. (2013)
7	2. 5 g	DMSO extraction method	Stirred 14 times the amount of DMSO at room temperature to avoid light for 30 min, impurity removal, filtered	The filter residue added DMSO to soaking, heating extraction in seal condition at 80°C for 50 min, filtered. Then residue again added 12 times the amount of DMSO, heating extraction in seal condition at 80°C for 50 min. Filtered and combined the filtrate	The filtrate added 3 times of the amount of butyl acetate, centrifuged. Washed the precipitate with ethanol, dried	14.564%	A comparation of hot, cold and ultrafiltration models	Li et al. (2016)

TABLE 2 | Summary of the detection methods of HSYA.

No	Methods	Sample source	Sample preparation	Chromatographic method details	Advantage	Reference
1	HPLC-DAD and UPLC-Q-TOF-MS	Plant extracts	Dried in the cabinet drier at 35°C for 24 h, crushed and passed through an 80-mesh sieve and stored in a desiccator at room temperature	Waters ACQUITY BEH C18 column (30.0°C), elution solvent: Methanol: Water (1: 3, v: v) And flow-rate of 0.8 ml/min	High-speed separation and structural identification of multiple constituents	Hong et al. (2015)
2	UFLC-Q-TOF/MS	Bile, urine, plasma and feces samples from SD rat	Mixed sample at same time point, loaded onto a SupelClean™ LC-18 SPE tube	Thermo hypersil gold C18 column (35.0°C), elution solvent: Phase gradient, methanol A and 0.5‰ acetic acid in water B, flow rate of 0.2 ml/min	NA	Jin Y.et al. (2016)
3	LC–MS/MS	Human plasma	Mixed with internal standard working solution and vortexed for 30 s	Shim-pack VP-ODS C_{18} column (30.0°C), isocratic elution system: Methanol and 5 mM ammonium acetate (80:20, v/v), flow rate of 0.4 ml/min	High selectivity, wide linear range, short run time (5.5 min per sample), low LOQ and small injection volume	Wen et al. (2008)
4	LC-MS/MS	Human plasma	Added to an internal standard working solution, vortexed and centrifuged, the supernatant loaded to the activated SPE solid phase cartridge, and then washed with water	Agilent ZORBAX SB C18 column (4.6 mm × 150 mm, 5 μm, 35°C), elution solvent: 0. 2 mol L^{-1} ammonium acetate aqueous solution/ methanol (30/70), flow rate of 400 μL/min	NA	Li et al. (2014)
5	UPLC–MS–MS	Human urine	Freeze-dried, added 10% perchloric acid and 1 ml ethyl acetate, centrifuged, and dried under uitrogen gas blower	UPLC BEH C18 column (2.1 × 100 mm, 1.7 μm), elution solvent: Gradient elution, Acetonitrile-0.5% acetic acid (42:58), flow rate of 0.35 ml/min	NA	Zeng et al. (2013)
6	UPLC-DAD–MS	Xue fu zhu yu (XFZY)	Pills and granules of XFZY ground to fine powder, separated by 50% methanol–water solution extraction. Liquids of XFZY, 1 ml was diluted to 50 ml by 50% methanol–water solution	ZORBAX SB-C18 column (4.6 mm × 100 mm, 1.8 m): (50.0°C), mobile phase: 0.1% formic acid–water A and acetonitrile B, gradient program, flow rate of 0.5 ml/min	High-speed detection, excellent peak shapes, and less solvent usage	Zhang et al. (2012)
7	RP-HP LC-UV	Xuebiqing injection	XBJ injection of 1.0 ml was diluted to 10 ml with millipore water and filtered through 0.45 mm membrane filters	Zorbox SB C18 column, elution solvent: Gradient elution, water with 0.2% phosphoric acid A and acetonitrile B, flow rate of 1.0 ml/min	Better biocompatibility, larger specific surface area, good conduction effect and catalytic activity	Wang et al. (2016)
8	Novel multilayered porous silicon-based immunosensor	NA	Synthesized the polyclonal anti-HSYA antibody and HSYA artificial antigen by the immediate coupling method	NA	High surface area, easily preparation, label-free procedures and compatibility with standard microelectronics processing	Lv et al. (2011)

chloroform. So, the most general and traditional extraction method to get HSYA is water immersion. However, water immersion has the characteristic of low yield and high consumption of raw materials (e.g., the yield of 0.023%, 800 g of safflower; the yield of 0.066%, 2000 g of safflower) (Bai et al., 2012; Li et al., 2013a). Simultaneously, high temperature, alkaline conditions, and illumination all accelerate the degradation of HSYA in the traditional procedure.

As shown in **Table1**, many other extraction systems were developed. Smashing tissue extraction holds an absolute advantage in time consumption compared with other extraction systems, with a yield of 1.359% in two minutes (Wang et al., 2012). MAS-I microwave extraction system with a solid and liquid ratio of 100 maintained at 70°C for 3 cycles in 20 min could obtain HSYA with higher yield of 6.96% (Yang et al., 2008). Hong et al. (2015) compared the effectiveness of MSPD, ultrasound extraction, and Soxhlet extraction methods. MSPD system obtained the highest yield at 14.89% compared with ultrasonic (12.25%) and Soxhlet extraction (13.09%), and also achieved the lowest consumption of raw materials.

Solvents also affect the extraction efficiency. Li et al. (2016) developed the DMSO extraction method as follows: Soak 2.0 g safflower with 14 volumes DMSO and stir for 30 min to remove impurities at room temperature in dark environment. Then soak the filter residue with 14 volumes of DMSO at 80°C for 1 h before heating for 50 min in the same environment. Soak the filter residue with another 12 volumes DMSO and repeat the steps above. Then add 3 volumes butyl acetate to the filtrate and centrifuge to obtain crimson precipitates. Finally, wash the precipitates with an appropriate amount of ethanol before drying to obtain light yellow powder with yield at 14.56%. DMSO is a "universal solvent" in areas of pharmaceutical sciences and cell biology, so it is inevitable to dissolve a lot of impurities during the extraction process, and the toxicity of DMSO is difficult to remove. Therefore, this method is not recommended to be extensively promoted.

Detection Methods

Several detectors coupled with a liquid chromatography (LC) system have already been used for HSYA detection, including diode (DAD) (Qi et al., 2007), electrochemical (ECD), mass spectrometer (MS), and ultraviolet (UV). In addition, the novel multilayer porous silicon-based immunosensor has also been applied for HSYA detection. Detailed information is provided in **Table 2**.

MS is the most effective detector for qualitative analysis of HSYA with a high detection sensitivity, selectivity and low-interference. HSYA and its metabolites can be accurately identified, based on mass-to-charge ratio (m/z) and fragmentation patterns.

The content of HSYA in human plasma was determined after oral administration of safflower. LC-MS/MS method with isocratic elution system composing of methanol and 5 mM ammonium acetate (80:20, v/v) was proved with a linear range of 1–1,000 ng/ml, a correlation coefficient ≥0.999 (Wen et al., 2008). Li et al. (2014) optimized the sensitivity and selectivity of this method to be more simplified and effective. The researchers replaced the Thermo syncronis C8 with Agilent ZORBAXSB C18, added ammonium acetate to the mobile phase and increased concentration dilution ratio. The modified method reduced the injection volume, improved the response intensity and peak shape, and shortened the retention time.

UPLC-DAD-MS method had the advantages of fast detection speed, good peak shape and less solvent consumption. Twenty-eight compounds were identified only in 30 min, including HSYA from Xue Fu Zhu Yu decoction, a classic prescription of TCM (Zhang et al., 2012).

UPLC-TOF-MS is the most powerful tool with accurate activity measurement and full spectral sensitivity to determine HSYA using gradient elution with acetonitrile and 0.1% (v/v) formic acid aqueous solution in ESI^+. This method showed good linearity ($r^2 \geq 0.9992$) and precision (RSD ≤3.4%) with the limits of detection (LOD) at 35.2 ng/ml (Hong et al., 2015). Jin et al. (2016b) successfully developed a UFLC-Q-TOF-MS method to detect HSYA and its multiple metabolites in the plasma, bile, urine and feces of SD rats after oral administration with HSYA using the mobile phase consisting of methanol and 0.5‰ acetic acid in water.

The analysis speed of UV detector for HSYA is very fast, but its sensitivity and selectivity are slightly weaker than that of MS system (Chen et al., 2010). Novel multilayer porous silicon-based immunosensor is an easy way to alter the etching current periodically, which fabricated of *p*Si photonic crystal. The linear relationship was ranging from 1 to 3 g/ml and detection limit at 0.78 ng/ml for HSYA detection (Lv et al., 2011).

PHYSICOCHEMICAL PROPERTIES

Physical Properties

HSYA, a C-glucosyl quinochalcone, is a yellow amorphous powder with a molecular formula of $C_{27}H_{32}O_{16}$ (Meselhy et al., 1993). It is usually used as a dye owing to its attractive color. It shows maximum absorption at 403 nm due to *p*-conjugated system coupled with several hydroxyl groups (Ma et al., 2014). The C-glycoside bond, located between the 1,3-diketone on the ring A, is unstable in HSYA. The hydroxyl group located at the C-2 position in the glycoside is easily condensed with the adjacent enol due to the strain effect. The pyranose ring is opened, and then forms an oxyfuran [3,2 days] benzofuran ring by a cyclization reaction (Suzuki et al., 2017). HSYA is easily degraded by light, high temperature, and alkaline conditions. HSYA emits weak fluorescence at 450 nm in aqueous solution owing to the lack of rigid planar configuration in the molecular structure, and borax can significantly increase the HSYA fluorescence intensity by 20 times (Cao et al., 2020). Due to the existence of phenolic hydroxyl groups, HSYA exists in protonated form in natural or alkaline aqueous solutions, which seriously affects its transmembrane ability and leads to low bioavailability.

Chemical Stability

Effect of pH

HSYA is easy to degrade under alkaline conditions. Pu et al. (2017) had illustrated the pH profile (1–14) of HSYA stability in

aqueous solution follows an inverted V curve, and it was most unstable at pH 9. When HSYA was transferred from the aqueous solution to the buffer solution at pH 9.16, the UV absorbance was red-shifted from 404 nm to 426 nm, with the gradually increased absorbance of degradation products at 300 and 380 nm, which indicated that the electron cloud density of the conjugate system increased after rapid ionization under alkaline conditions.

As shown in **Figure 3**, there were two degradation products proposed in HSYA aqueous solution. The hydroxyl group at C-2′ was ionized under the moderate solution (pH 7–9). Intramolecular nucleophilic attacks Cβ and add O_2 to the α, *ß*-unsaturated double bond. The two products are isomers, which obtained after hydrogen migration. There were chalcone, flavones, and carbanion intermediates detected in HSYA acidic neutral and aqueous solution. However, only flavones were found under strong alkaline conditions (pH 13).

Effect of Temperature

When HSYA was incubated in boiling water under dark conditions for 0, 0.5, 1, 2, and 4 h, the degradation rate of HSYA was increased gradually detected by HPLC system. The possible mechanism of HSYA degradation was that the colorless glycoside of HSYA bonded with H_2O to form conjugate system, which reacted with the adjacent enol to transform the chromophore structure under the high temperature (Yue et al., 2003; Li et al., 2009). HSYA can be directly hydrolyzed and transformed into *p*-coumaric acid. And the hydroxyl group at the 2-position of C-glycoside of HSYA can be also condensed with the adjacent enol on A ring, and oxidized by O_2 at pH 8 under the high-temperature condition, then obtained the degradations (**Figure 4**). Due to the instability of the degradations as enols, a mixture of the two degradations were obtained (Fan et al., 2011).

Effect of Light

HSYA degrades when exposed to light, so it is generally stored in dark conditions. When distilled water solution of HSYA was exposed under sunlight, ultraviolet, incandescent light, and the dark environment respectively, the content of HSYA decreased in turn analyzed by HPLC (Li et al., 2011). The content of HSYA in aqueous solution decreased when stored under natural light at room temperature for 20 days (Wang, 2017).

Effect of Fe^{3+}/Fe^{2+}

When HSYA was incubated with Fe^{3+} (0.1 μg/ml) or Fe^{2+} (0.05 μg/ml) at 60°C for 10 h, the multiple nucleophilic hydroxyl groups and carbonyl groups of HSYA combined with Fe^{3+} and Fe^{2+} to form chelate compounds, leading to accelerate degradation of HSYA. Ethylenediaminetetraacetic acid (EDTA) competes with Fe^{3+} or Fe^{2+} to reduce HSYA degradation (Wang, 2017).

DRUG DELIVERY SYSTEM

A drug delivery system is responsible to control the release rate, extend the duration of drug action, and eliminate side effects, which can be divided into 4 types, including lipid-based carriers, polymer nanoparticles, inclusion complexes, and capsulations. At present, the studies on the HYSA drug delivery systems mainly focuses on lipid-based carriers, which can improve the bioavailability by reducing the high-water solubility of HSYA. Moreover, microemulsions, self-emulsifying systems, and nanoparticles can also enhance the transmembrane capacity of HSYA. In this review, we also summarized other drug deliveries, such as chitosan, and the combination of HSYA with other drugs. A detailed description is provided in Ahmed and Aljaeid, 2016, **Figure 5**.

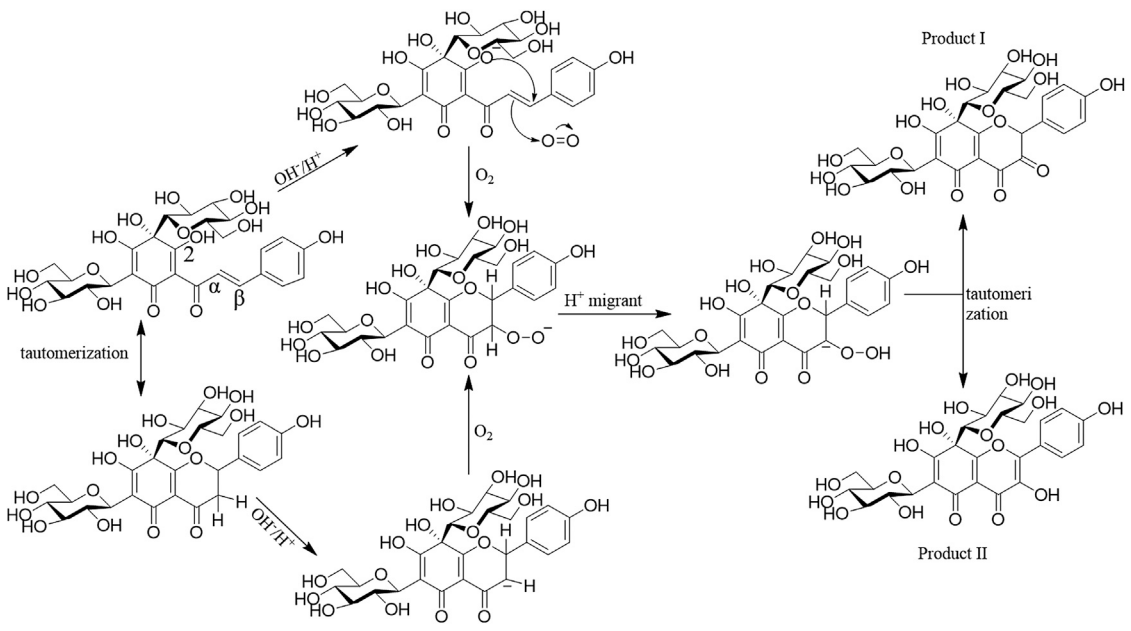

FIGURE 3 | The pathway of HSYA degradation (Pu et al., 2017).

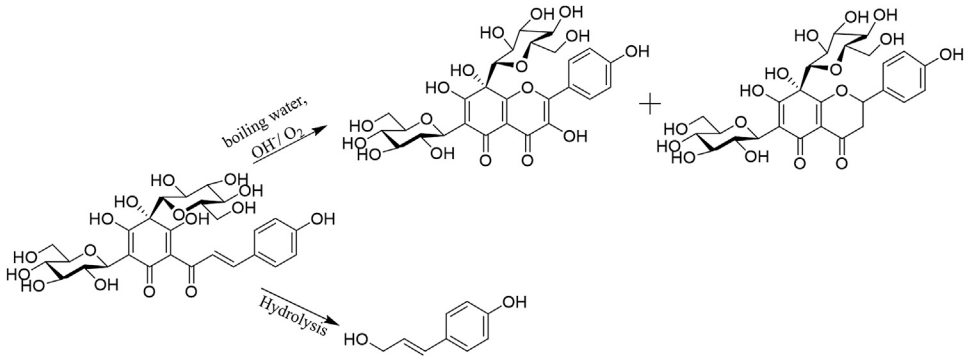

FIGURE 4 | Proposed degradation pathways of HSYA in the buffer solution at pH 8.0 at 100°C.

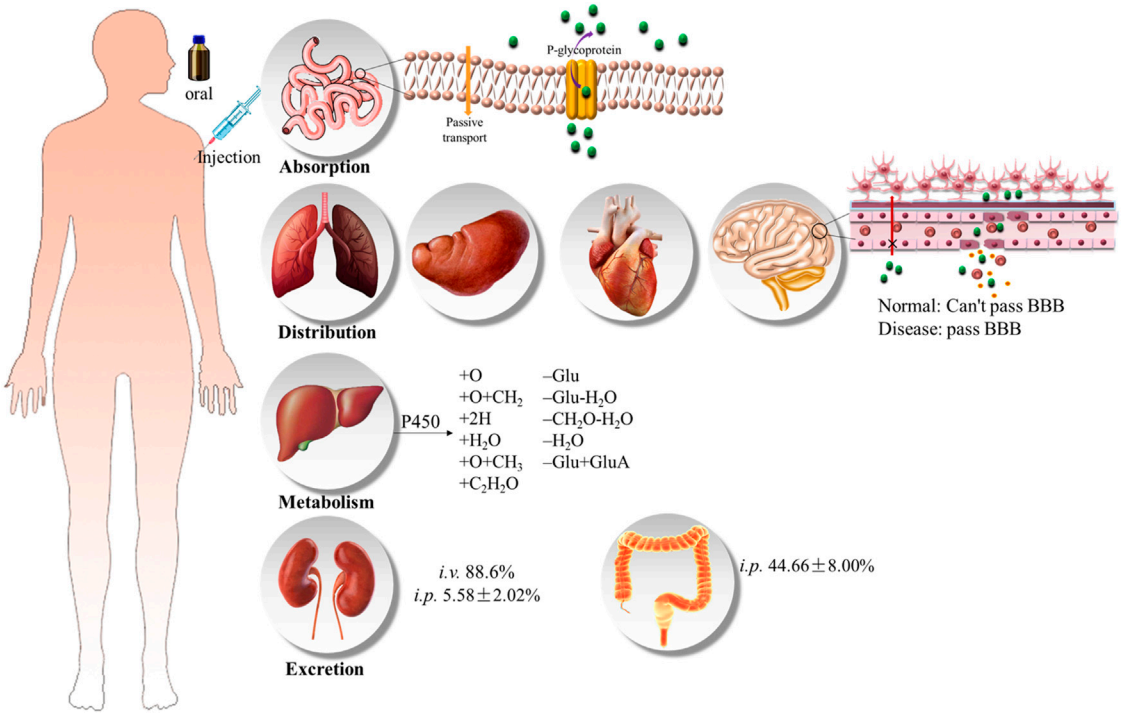

FIGURE 5 | Scheme of the pharmacokinetics of HSYA.

Microemulsions

Microemulsions are stable liquid solution consisted of water, oil, surfactant, and co-surfactant, with the characteristic of isotropic and thermodynamics. They are transparent or translucent with small droplet size, typically up to 150 nm (Lopes et al., 2014; Lv et al., 2018). Microemulsions are used to increase the permeability of hydrophilic peptides by enhancing the fluidity of cell membranes and opening tight connections between cells, which is a potential tool for hydrophilic drug molecules. Qi et al. (2011) investigated the bioavailability of HSYA microemulsion by intraduodenally administration. The microemulsion of HSYA was prepared by mixing Cremophor RH40 (surfactant), ethanol (cosurfactant), and PG (oil phase) together. Compared with HSYA aqueous solution, the bioavailability of HSYA microemulsion was increased by almost 1937%. It is worth noting that bile has a significant effect on the absorptive capacity of microemulsions. The microemulsion showed lower enhanced bioavailability of only 181% in bile duct-ligated rats. Microemulsion digested by pancreatic lipase increased 5.56 times permeability than the diluted microemulsion. The lipids and surfactants in the HSYA microemulsion might increase the fluidity of cell membranes and open the tight junctions between cells, thereby improving the permeability of hydrophilic drug molecules.

Self-emulsifying drug delivery system (SDEDDS) is a kind of the microemulsions. It could rapidly and spontaneously form a microemulsion in the gastrointestinal tract, where the peristalsis of the gastrointestinal tract and small intestine provides the necessary agitation for emulsification. SDEDDS have multiple advantages, including 100% drug entrapment capacity, physically stable formulations, no dissolution required, and submicron droplet sizes (Ghasemiyeh and Mohammadi, 2018). SDEDDS of HSYA were synthesized by inner water phase of 0.5% gelatin solution, and the external oil phase of bean phospholipids, medium chain triglycerides, Tween 80, oleic acid, and labrasol (20/65/7.4/2.5/0.1, in wt%). The study demonstrated that SDEDDS significantly improved the permeability of HSYA through Caco-2 cells monolayers, and plasma concentration increased by 2.17 times. The apparent permeability coefficient (Papp) of HSYA and HSYA-SDEDDS were (3.52 ± 1.41) × 10^{-6} cm/s and (6.62 ± 2.61) × 10^{-6} cm/s at the same concentrate (0.4 mg/ml), which improved to 1.88-fold by SDEDDS (Lv et al., 2012).

Labrafac lipophilic WL1349 (WL1349) is a medium-chain triglyceride that can be digested, absorbed, and hydrolyzed by pancreatic lipase after being emulsified by an endogenous emulsifier (such as bile). Preparation of HSYA-phospholipid complex increased lipophilicity, and dissolved in WL1349 to form a stable oil solution (a lipid-based preparation). Compared with HSYA aqueous solution, the oral bioavailability of HSYA-phospholipid complex WL 1349 oil solution in rats increased by about 37 times (Cmax of 2.79 μg/ml vs. 0.08 μg/ml within 24 h) and reduced the excretion of the drugs (8.80 ± 2.30% vs. 44.66 ± 8.00% in feces within 24 h) (Wang et al., 2008; Li et al., 2010a).

Nanoparticles

Solid lipid nanoparticles (SLN) is the earliest lipid-based nanocarriers formulated from lipids with a submicron size less than 1,000 nm, which are solid at body temperature and stabilized by emulsifiers (Koga et al., 2010). They can protect drugs against harsh environmental and are easy to mass-produce. However, owing to the crystalline structure existed in SLN, the drug-loading efficiency is poor. Some of the main lipids that have been used so far are monostearic acid, stearyl alcohol, stearic acid, glyceryl monostearate, cetyl palmitate, poloxamer 188, Tween 80, and dimethyl octadecyl ammonium bromide (DDAB) (Lee et al., 2016; Tapeinos et al., 2017; Ghasemiyeh and Mohammadi, 2018). As reported by Zhao et al. (2017), 1% Tween 80 was used as an emulsifier. HSYA-SLN with w/o/w structure prepared by micro emulsification procedure significantly improved oral bioavailability. HSYA SLNs is spherical with an average diameter of 174 ± 20 nm, zeta potential of −12.4 ± 1.2 mV, and the encapsulation efficiency is 55%. The SLNs of HSYA were stable within ten days at 4 or 30°C. SLNs of HSYA increased the oral bioavailability of HSYA in rats about 3.97-fold. It also significantly enhanced the C_{max} and AUC by 7.76 and 3.99 folds. The pharmacodynamic evaluation showed that HSYA-SLNs had a better therapeutic effect on the cerebral ischemia rats compared to HSYA aqueous solutions (Zhao et al., 2018).

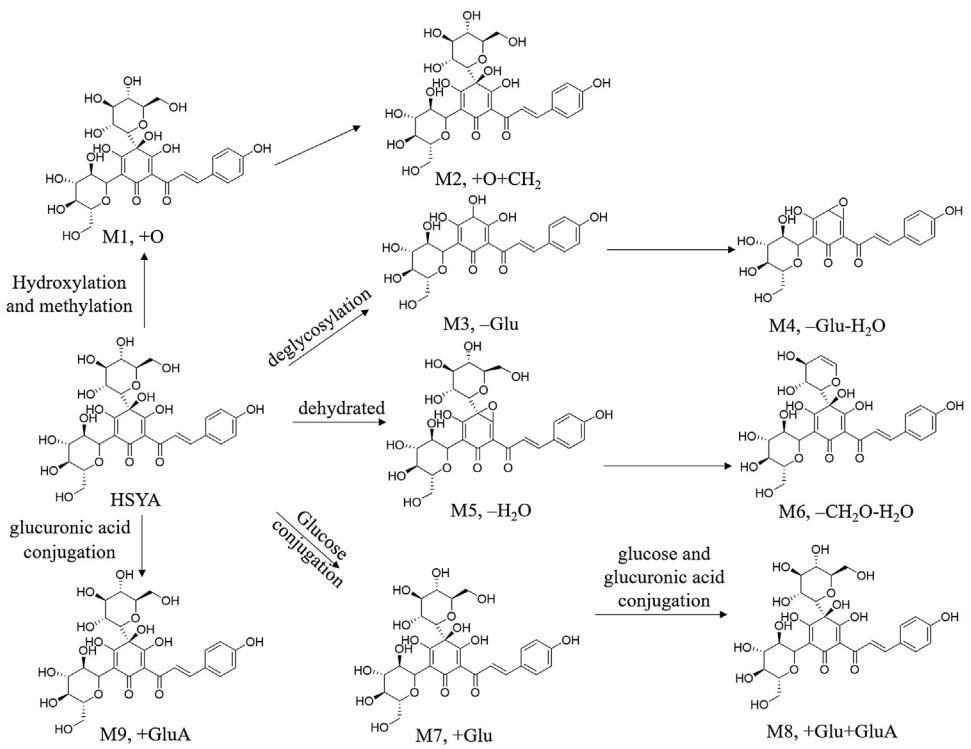

FIGURE 6 | Proposed metabolic pathways of HSYA (Jin et al., 2016; Wu et al., 2018).

Others Delivery System

The combination of *Ligusticum* chuanxiong volatile oil (CVO) and HSYA also improved the bioavailability in rats. When HSYA co-administered with CVO of 0.02 mg/ml, the bioavailability of HSYA in rats was increased by 6.48 folds. The emulsification of CVO increased Papp of HSYA and the paracellular transport by opening the integral tight junction of Caco-2 cells.

Chitosan, a kind of biological polysaccharide, is a molecule usually obtained by deacetylation of chitin with the carbohydrate backbone structure similar to cellulose, which is composed of two kinds of repeating units, N-acetyl-D-glucosamine and D-glucosamine, combined with (1–4)-β-glucoside linkage. It is characterized by the presence of a lot of amino groups on the chain (Ahmed and Aljaeid, 2016; Hong et al., 2017). HSYA-Chitosan complex effectively improved the oral absorption of HSYA, and the bioavailability increased to 476% (Ma et al., 2015).

Drug delivery system has great potential to improve the bioavailability and chemical instability of HSYA. However, there are also some several challenges, such as high preparation cost and poor promotional effect, which need further improvement.

PHARMACOKINETICS

HSYA is one of the representative chemical compounds of biopharmaceutics classification system (BCS) class III drugs. Pharmacokinetic studies showed that HSYA had low bioavailability. The oral bioavailability of HSYA is only 1.2%, and 48% of the prototype drug is excreted in urine, 2.9% in feces, and only 0.062% ± 0.011% in bile (Zhang, 2006). Similarly, 88.6% was directly excreted through urine after intravenous administration (Sun et al., 2009) (Ahmed and Aljaeid 2016, **Figure 6**).

Caco-2 cell monolayer model was usually used to study the transmembrane characteristic of HSYA, and the result prompted that the absorption of HSYA is basically in line with the passive diffusion. P-gp inhibitors (verapamil) and energy metabolism inhibitors (sodium azide) failed to block the intake of HSYA, which demonstrated that the absorption of HSYA is irrelevant to the P-gp protein (Zhou et al., 2014). However, this conclusion needed more evidence to verify owing to the opposite result in another study (Wang et al., 2009). The peak concentration of HSYA generally appeared at 10 min after oral administration (Li et al., 2007). A study has shown that healthy volunteers received intravenous injections of 35, 70, and 140 mg of HSYA, the elimination half-life values ($t_{1/2}$) of HSYA was 3.32 h, and the C_{max} was (2.02 ± 0.18), (7.47 ± 0.67), (14.48 ± 4.70) mg L^{-1}, respectively, (Qiao et al., 2009). HSYA has a low plasma protein binding rate (48%–54.6%, 72 h, *i. v.*), and it has no competitive binding to other drugs. So, HSYA is highly safe *in vivo* (Chu et al., 2006). Yang et al. (2009) suggested that the therapeutic effect of the single-dose HSYA indicated proportional to the dose ranging from 35 to 140 mg/kg, which conformed to first-order kinetics in

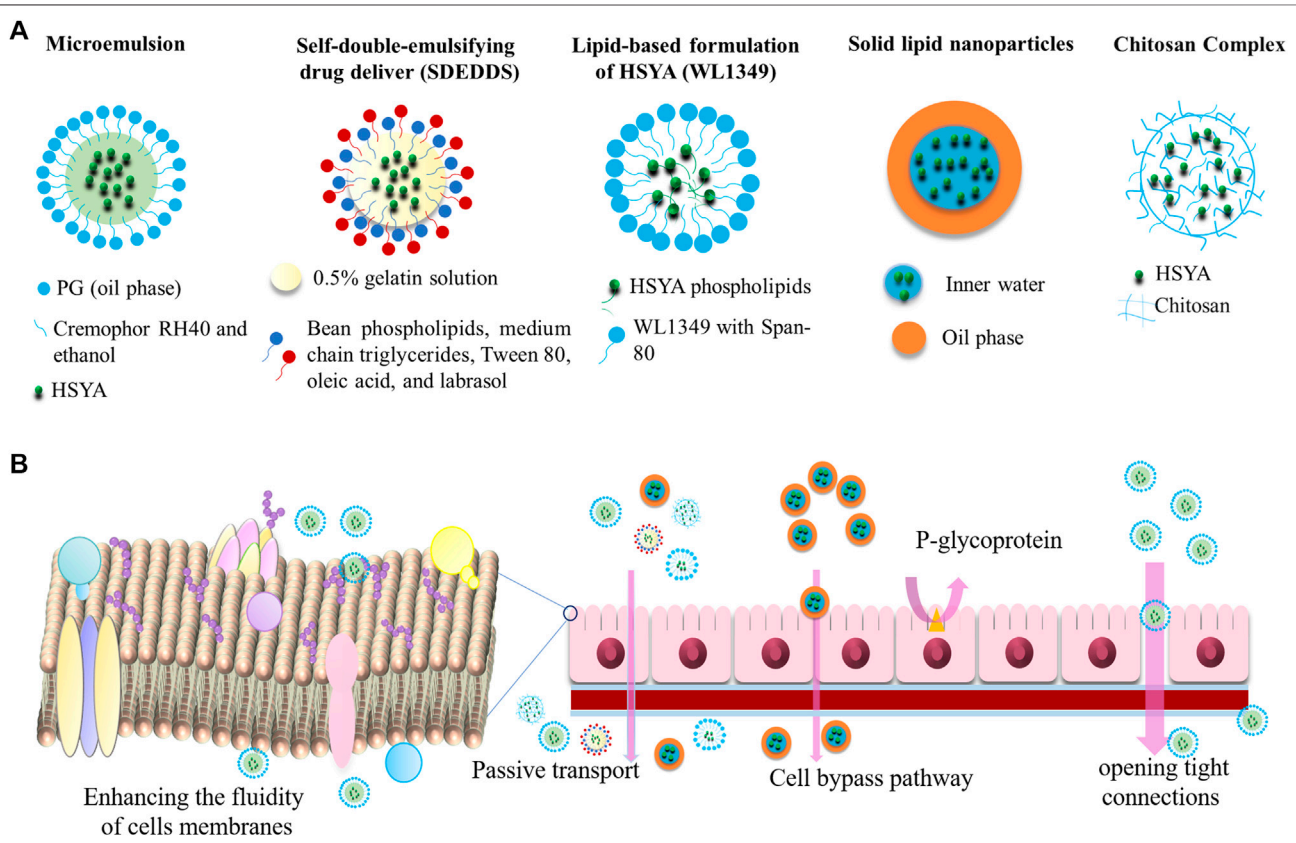

FIGURE 7 | Schematic representation of the different kinds of colloidal delivery systems.

TABLE 3 | Pharmacological effects of HSYA.

Pharmacological effects	Species	Study model	Detail	Effective concentration/dose/pattern	Remark	References
Cardioprotective effects	*In vivo*: SD rats	LAD of the coronary artery ligation	Reduce the myocardial infarct size (MIS), decrease CK-MB, MDA, increase eNOS, SOD, NO	HSYA + NTG (10 mg/kg+0.3 mg/kg)	HSYA combined with NTG	Wang et al. (2017)
	In vivo: SD rats *In vitro*: H9c2 cells	*In vivo*: isoproterenol-induced myocardial injury *in vitro*: Oxygen–glucose deprivation (OGD) model	Reduce the levels of CK-MB, ROS, LDH, inhibit apoptosis, increase PGC-1α and Nrf2	*In vivo*: HSYA + AKBA (50 mg/kg+50 mg/kg) via intragastric tubes. *In vitro*: HSYA + AKBA (5 μM + 5 μM)	HSYA and AKBA	Chen et al. (2016)
	In vitro: Cells from SD rats	Hypoxia/Reoxygenation (H/R)	Enter the cardiac myocyte and able to modulate H/R-induced damage by interacting with the MPTP	200 μM	NA	Huber et al. (2018)
	In vivo: SD rats	Ischemia–reperfusion (I/R) langendorff apparatus model	Inhibit MPTP opening, enhance nitric oxide production	0.05, 0.1 mmol/L	NA	Liu et al. (2008)
	In vivo: Wistar rats, TLR4-knockout C57 mice *in vitro*: NRVMs cells	*In vivo*: Hyperlipidemia combined with MI/R model. *In vitro*: LPS injured	Alleviate myocardial inflammatory injury, decrease MIS, CK-MB, LDH, LPS, TNF-α and IL-1β ability	Wistar rats: 8, 16, 32 mg/kg. TLR4-knockout mice: 16, 32, 64 mg/kg	NA	Han et al. (2016)
	In vivo: SD rats. *In vitro*: H9c2 cells	*In vivo*: LAD of the coronary artery ligation. *In vitro*: H/R model	Decrease apoptosis, improve antioxidant capacity, decrease the releases of cTnI, IL-6. LDH, and JAK2/STAT1 activity, maintain MMP, decrease ROS generation	*In vivo*: 5 mg/kg (*i.p.*). *In vitro*: 20 μM	NA	Zhou et al. (2019)
	In vitro:BV2 cells	OGD model	Decrease 1L-1β, TNF-α, iNOS, COX-2, MCP-1ability, inhibit NF-κB ability, phosphorylation of p38	20, 40, 80, 160, 320, 640, and 1,280 μM	NA	Li et al. (2013)
	In vivo: Male C57 mice. *In vitro*: HUVECs cells	*In vivo*: LAD of the coronary artery ligation	Improve ischemia-induced cardiac hemodynamics, enhance the survival rate, alleviate the myocardial injury, increase the level of CD31, VEGF-A and nucleolin	25 mg/kg (*i.p.*) twice a day for 2 weeks	NA	Zou et al. (2018)
	In vivo: SD rats. *In vitro*: H9c2 cells	*In vivo*: LAD of the coronary artery ligation. *In vitro*: H/R injury	Reduce CK-MB, cTnI, MDA and 8-OHdG, enhance SOD, Nrf2 and HO-1	1, 10, 35, 60, and 80 μM DSS + HSYA	Danshensu (DSS) and HSYA	Hu et al. (2016)
	In vitro: H9c2 cells	*In vitro*: H/R injury	Improve cardiomyocyte viability, maintain mitochondrial membrane potential, reduce apoptotic cardiomyocytes, decrease caspase-3 activity, and inhibit NOD-like receptor 3 (NLRP3) inflammasome activation through the AMPK signaling pathway	12.5 μM for 4 h	NA	Ye et al. (2020)
	In vivo: SD rats	*In vivo*: LAD of the coronary artery ligation	Reduce MIS, inhibit CK-MB and MDA content, increase SOD, eNOS and NO	2, 4, or 8 mg/kg via the tail vein injection	NA	Tu et al. (2009)
Neuroprotective effect	*In vivo*: Male C57BL/6 mice	*In vivo*: MCAO model. *In vitro*: OGD/R model	Reduce ROS, suppress cellular apoptosis, promote mitochondrial function and biogenesis	*In vivo*: 5, 20 mg/kg for 3 days. *In vitro*: 1, 10 μM	NA	Chen et al. (2019)
	In vivo: Wistar rats. *In vitro*: PC12 cells	MCAO/R model	Attenuate pressure overloaded hypertrophy, inhibit platelet aggregation, NF-κB p65 nuclear translocation, p65 binding activity, ICAM-1 and the infiltration of neutrophils	8, 4, 2 mg/kg (*i.v.*)	NA	Sun et al. (2010)
	In vivo: SD rats	MCAO model	Protect cognitive function and synaptic plasticity, promote learning and memory ability	8, 16 mg/kg via common carotid artery (CCA) injection	NA	Yu et al. (2020)
	In vivo: Wistar rats	MCAO model	Decrease neurological deficit scores, reduce the percentage of infarction, attenuate MDA content, increase SOD and the T-AOC activity	2, 4, 8 mg/kg (*i.v.*)	NA	Wei et al. (2005)
	In vivo: C57BL/6J mice	MCAO model	Inhibit TLR4, NF-κB, p-p65 expression, ERE1/2, JNK and p38 phosphorylation, suppressed TNF-α, IL-1β, NO	2 mg/kg via the tail vein injection	NA	Lv et al. (2015)
	In vivo: SD rats	MCAO/R model	Increase GFAP, NGF and Bcl-2 expression, suppress the expression of bax, caspase-3 and ICAM-1, IL-1ß, TNF-α and NF-κB	10 mg/kg HSYA+300 mg/kg acetylglutamine (NAG) once each day for 7 days	HSYA and NAG	Deng et al. (2018)
	In vivo: SD rats. *In vitro*: Cortical neurons cells	*In vivo*: MCAO model. *In vitro*: OGD model	Decrease LDH, TNF-α, IL-1β and IL-6, increase SOD, MDA, GSH-Px, suppress TLR4 and NF-κB expression, enhance Nrf2 and HO-1 expression	*In vivo*: 7.5 mg/kg+3 mg/kg (DSS + HSYA). *In vitro*: 40 μM + 40 μM (DSS + HSYA)	HSYA and DSS	Xu et al. (2018)
	In vivo: Male C57BL/6 mice	NA	Prevent the appearance of motor abnormalities, attenuate the reduction of dopamine (DA), 3,4-dihydroxyphenylacetic acid (DOPAC) and homovanillic acid (HVA) in striatum	2, 8 mg/kg for five days (*i. v.*)	NA	Han and Zhao (2010)
	In vivo: C57/BL6 mice	Rotenone-induced PD model	Increase the expression BDNF, *p*-TrkB/TrkB, DRD3, p-PI3K/PI3K, *p*-AKT/AKT, improve motor dysfunction	20 mg/kg for 28 days	NA	Wang et al. (2017)
	In vivo: SD rats	Unilateral 6-OHDA lesion (PD model)	Increase the levels of dopamine and its metabolites, glial cell line-derived neurotrophic factor and brain-derived neurotrophic factor	2 or 8 mg/kg via caudal vein injection for 4 weeks	NA	Han et al. (2016)
	In vivo: SD rats	Hcy-induced AD model	Attenuate ab accumulation, improve synaptic function, and reversed hcy-induced cognitive impairment	6 mg/kg (*i.v.*) for 2 weeks	NA	Lu et al. (2013)

(Continued on following page)

TABLE 3 | (*Continued*) Pharmacological effects of HSYA.

Pharmacological effects	Species	Study model	Detail	Effective concentration/dose/pattern	Remark	References
	In vivo: Wistar kyoto (WKY) rats	MCAO model	Increase the ratio of 6-keto-PGF1a and TXB2	1.5, 3.0, 6.0 mg/kg via sublingular vein injection	NA	Zhu et al. (2015)
	In vivo: SD rats	MCAO model	Inhibit protein oxidation and nitration, 12/15 lipoxygenase (12/15-lox), oxidative stress, attenuate BBB breakdown, infarct volume, BBB permeability, and brain edema	1, 5 and 10 mg/kg via caudal vein injection	NA	Sun et al. (2012)
	In vivo: Wistar rats	Cervical lymphatic blockade model	Alleviate the neurological deficits, attenuated cell apoptosis, prevent the decrease of eNOS mRNA and protein expression	5 mg/kg, (*i.p.*)	NA	*Pan* et al. (2012)
	In vivo: SD rats	Isolate brain mitochondria of SD rat	Inhibit Ca^{2+}- and H_2O_2-induced swelling of mitochondria, improve mitochondrial energy metabolism, enhance ATP levels and the respiratory control ratio	10–80 μmol/L	NA	Tian et al. (2008)
	In vivo: SD rats	Vascular dementia (VaD) model	Reduce escape latency in the water maze, enhance the LTP at CA3-CA1 synapses, up-regulated both VEGF and NR1, promote angiogenesis and increase synaptic plasticity, improve spatial learning and memory	0.6 mg/100 g via tail-vein injection for two weeks	NA	Zhang et al. (2014)
	In vivo: SD rats	Traumatic brain injury	Increase superoxide dismutase activity, decrease MDA content, enhance the t-PA activity, decrease the PAI-1 activity, decrease the MMP-9 expression	4 mg/kg (*i.v.*)	NA	Bie et al. (2010)
	In vivo: SD rats and balb/c male mice. *In vitro*: PC12 cell line	*In vivo:* MCAO model. *In vivo*: H_2O_2	Reduce the volume of cerebral infarction, improve the histopathological morphology, recruit brain-derived neurotrophic factors, down-regulate NLRP3, ASC, Caspase-1, GSDMD, IL-1β, IL-18, LDH, NF-κB, and p-p56 expression	*In vivo*: 5, 10 and 20 mg/kg (*i.v.*)	HSYA with lexiscan	Tan et al. (2020)
	In vivo: Pregnant C57BL6 mice	LPS-induced neurotoxicity and neuroinflammation	Decrease the content of IL-1β, TNF-α and NO, attenuate the LPS-induced dopaminergic neurons damage, inhibit the expressions of NF-κB, p65 and iNOS, decrease the content of IL-1β, TNF-α and NO	0, 20, 40, 80, 160, 320, 640 μM	NA	Wang et al. (2018)
	In vivo: C57BL6 mice. *In vitro*. SH-SY5Y cells	*In vivo*: PD model (*6-hyroxydopamine*)	Reduce iNOS, COX-2 and NF-κB, attenuate neuronal apoptosis, reduce the levels of p-p38 and *p*-JNK and increase that of *p*-ERK	*In vivo*: 2, 4, or 8 mg/kg (*i.v.*). *In vitro*: 1, 5, or 10×10^{-6} mol/L	NA	Yang et al. (2020a)
	In vivo: Wistar rats. *In vitro*: Primary neuronal cells	*In vivo*: MCAO model. *In vitro*: OGD model	Reduce infarct volume, decrease neurological deficit scores, elevate. GSK3β phosphorylation and inhibite the activation of iNOS, NF-κB, and capase-3	*In vivo*: 2, 4, or 8 mg/kg (*i.v.*)	NA	Yang et al. (2020b)
	In vitro: Human brain microvascular endothelial cells (HBMEC)	Methylglyoxal (MGO)-induced injury	Inhibit MGO-induced cell apoptosis, attenuate AGEs accumulation	10–100 μmol/L	NA	Li et al. (2013)
–	*In vivo*: SD rats	MCAO/R model	Promote neurological and functional recovery, suppress JAK2/STAT3 activation, activate of SOCS3	4, 8 or 16 mg/kg injected via the unilateral common carotid artery of rat	NA	Yu et al., 2020
–	*In vivo*: SD rats	A rat model of vascular dementia	Reduce escape latency in the water maze, promote angiogenesis and increase synaptic plasticity, improve spatial learning and memory, increase VEGF-A expression, protect neurons against hypoxia, increase NR1 expression, promote LTP and increase synaptic plasticity	0.6 mg/100 g for two weeks via tail-vein injection	NA	Zhang et al., 2014
Anticancer effect	*In vivo*: BALB/c mice. *In vitro*: Hepa1-6 murine HCC cells	A mouse model of hepatocellular carcinoma	Inhibit the proliferation of liver cancer cells, reduce the extent of tissue damage induced by cisplatin, increase the thymus index of HCC model mice, reduce the expression of Foxp3 and roryt mRNA, improve the tumor immune microenvironment of HCC model mice	2.25, 1.13 and 0.57 mg/kg twice per day (*i.v.*) for 11 days	NA	Ma et al., 2019a
	In vitro: Human umbilical vein endothelial cell (HUVEC)	High-glucose induced HUVEC injury	Attenuate cells apoptosis, decrease hyperpermeability, inhibit ROS levels	0–50 μM	NA	Chen et al. (2019)
	In vitro: Skov3 cells	NA	Decrease ovarian cancer cell proliferation, decrease ovarian cancer cell viability and sensitizes cells to chemotherapeutic agents, downregulate WSB1 expression	0, 10, 20, 50, 100, and 150 mg/L for 72 h	NA	Ma et al., 2019b
	In vitro: KYSE-30 cells	NA	Suppress proliferation, invasion, and migration, simultaneously induce apoptosis, regulate NF-κB signaling pathway, ICAM1, MMP9, TNF-α, and VCAM1	0.1, 1, 10, 20, 50 μM	NA	Chen et al. (2020)
	In vivo: Kunming mice. *In vitro*: HepG2 cells	H22 liver cancer cells injected into the abdominal cavity of kunming mice	Suppress p38MAPK phosphorylation, decrease HepG2 cell viability, proliferation, and migration, inhibit apoptosis of HepG2 cells	*In vivo*: 1.125 mg/kg, 2.25 mg/kg for 14 days (*i.v.*). *In vitro*: 80 μM	NA	Zhang et al., 2019

(Continued on following page)

TABLE 3 | (*Continued*) Pharmacological effects of HSYA.

Pharmacological effects	Species	Study model	Detail	Effective concentration/dose/pattern	Remark	References
Immunoprotection	*In vivo*: C57BL/6	Bleomycin-induced mice lung injury model	Attenuate the loss in body weight, alleviate bleomycin-induced increase of mRNA level of TNF-α, IL-1β and TGF-β1 in lung homogenates, inhibited NF-κB and phosphorylation of p38 MAPK in lung tissue	26.7, 40, 60 mg/kg/d (*i.v.*) for 1 week	NA	Wu et al., 2012
	In vivo: C57BL/6 mice	LPS-induced acute respiratory distress syndrome	Alleviate expressions of TNF-α, IL-1β, IL-6, TGF-β1, Col-I, col III, *a*-SMA, MD-2, TLR and CD14, inhibit the elevated levels of NF-κB and *a*-SMA, alleviated the slight collagen deposition in pulmonary tissues, attenuated increased levels of p65	14, 28, 56 mg/kg/d for 10 days (*i.v.*)	NA	Zhang et al., 2017
	In vivo: Hep-G2 liver cancer cell line	NA	Increase LC3-II and beclin 1 expression, decrease the level of p62 and phosphorylated-ERK1/2	20 mg HYSA solved in 1.02 ml PBS	NA	Liu et al., (2020)
	In vivo: ICR mice	LPS-induced acute lung injury (ALI)	Attenuate lung vascular permeability and edema, down-regulate myeloperoxidase (MPO), inhibited p38, ERK, JNK, TLR4, MyD88 and TRIF and the phosphorylations of interferon regulatory factor 3 (IRF3)	40, 80, and 120 mg/kg (*i.p.*)	NA	Liu et al., 2014
	In vivo: Specific-pathogen-free mature male hartley Guinea pigs	Ovalbumin (OVA)-induced asthma in Guinea pigs	Reduce airway resistance, improve dynamic lung compliance, attenuate the pathologic changes, inhibit the phosphorylation of JNK, p38, ERK, and IkBa, and inhibited IgE, PAF, IL-1b, IL-6, IL-4, IL-5, and IL-13 and increase in TNF-a, IFN-g, IL-2, and IL-3	50, 75, 112.5 mg/kg once daily from days 2–22 (*i.v.*)	NA	Zheng et al., 2019
	In vitro: Human non-small cell lung cancer cell line (A549)	LPS-mediated inflammatory injury	Suppress the expression of TLR-4, Myd88, ICAM-1, TNFα, IL-1β and IL-6, inhibit the adhesion of leukocytes, decrease NF-κB p65 nuclear translocation, inhibit the phosphorylation of p38 MAPK	1, 4 and 16 μmol/L	NA	Han and Zhao (2010)
	In vitro: A549 and H1299	LPS-mediated inflame matory injury	Suppress proliferation, migration, invasion, and EMT, inhibit the PI3K/Akt/mTOR and ERK/MAPK signaling pathways	5, 10, and 20 μM for two weeks	NA	Jiang et al. (2019)
	In vitro: Human bronchial smooth muscle cells (HBSMCs)	NA	Suppress MLC phosphorylation, inhibit the activation, block asthma-related signal transduction pathways, block the binding of PAF to the PAFR on the target cell membrane	9, 27, 81 μmol/L	NA	Guo et al. (2019)
	In vitro: Eahy926 human endothelium cell	LPS-induced endothelium inflammatory injury	Attenuate ICAM-1 and E-selectin mRNA levels elevation, phosphorylation of p38 MAPK, Jun MAPK, inhibit leukocyte adhesion to EC	1, 10 and 100 μ mol/L	NA	Jin et al. (2016)
	In vitro: Human small airway epithelial cells (HSAECs)	PAF-induced activation of HSAECs	Inhibit PAF-induced inflammatory activation, inhibit the PKC and MAPK signaling pathways, suppress the activities of NF-κB and AP1	9, 27, and 81 μmol/L	NA	Guo et al., 2018
	In vivo: Male NIH mice	Cecal ligation and puncture mouse model of sepsis	Improve sepsis induced immunosuppression via inhibiting $CD4^+$ lymphocytes apoptosis under septic conditions, upregulate the expression of Bcl-2 protein, inhibit protein expression of cytc, bax, cleaved caspase-3, and cleaved caspase-9	120 mg/kg (*i. v.*)	NA	Wang et al., 2017
Vascular dementia	*In vitro*: Mouse 3T3-L1 preadipocytes	NA	Inhibit the proliferation and adipogenesis of 3T3-L1 preadipocytes, increase hormone-sensitive lipase (HSL) mRNA expression and promoter activities, increase HSL promoter activity	1 mg/L	NA	Zhu et al., 2015
	In vivo: Wistar rats	PE (phenylephrine)-induced vascular constriction	Possess vascular relaxation effects, activate the KV channel in pulmonary vascular smooth muscle cells	10^{-9} M, 10^{-8} M, 10^{-7} M, 10^{-6} M, 10^{-5} M	NA	Bai et al., 2012
	in vivo: C57BL/6J mice. *in vitro*: HUVEC cells	Mouse hindlimb ischemia model	Increase the capillary-like tube formation and migration of HUVEC, increase phosphorylation of Tie-2, akt, and extracellular signal-regulated kinase 1/2, promote reperfusion of ischemic hindlimb tissue	*in vivo*: 6 mg/kg for 11 days via the tail vein. *in vitro*: 0, 1, 10, 50, and 100 μM for 24 h	NA	Chen et al. (2016)
	in vivo: Wistar-Kyoto (WKY) rats and spontaneously hypertensive rats (SHR). *in vitro*. HEK293cells	NA	Activate BKCa channels, inhibit Ca-L channels, reduce intracellular free Ca^{2+} level	*In vivo:* 1, 10 mg/kg. *In vitro:* 50 μM, 100 μM, 150 μM	NA	Wang et al. (2020)
	in vivo: Wistar rats. *In vitro:* Rat mesenteric endothelial cells (primary)	NA	Decrease TRPV4-dependent influx of Ca^{2+} in endothelium cells, promote PKA-dependent eNOS phosphorylation and increase NO production mechanism	*In vitro*: 10^{-7}, 10^{-6}, 10^{-5}, 10^{-4} M	NA	Yang et al. (2020)
	In vitro: HUVEC cells	NA	Inhibit the expression of VEGF and KDR, reduce Ras, *p*-raf, *p*-ERK and p-p38MARK, inhibit the expression of c-myc, N-ras, and NF-κB	NA	NA	Wang et al. (2016)

(Continued on following page)

TABLE 3 | (*Continued*) Pharmacological effects of HSYA.

Pharmacological effects	Species	Study model	Detail	Effective concentration/dose/pattern	Remark	References
Hepatoprotective effects	*In vivo:* C57BL/6 mice	D-galactose- (D-gal-) induced aging	Increase SOD, CAT, GSH-Px and MDA, decreased the mRNA and protein level of cyclin-dependent kinase inhibitor p16, increase CDK4/6 protein expression and decrease the phosphorylation of retinoblastoma (pRb)	25 mg/kg HSYA daily (*i.v.*) for 8 weeks	NA	Min et al. (2020)
Pulmonary arterial hypertension	*In vivo*: male wistar rats	A model of monocrotaline (MCT)-induced pulmonary arterial hypertension (PAH)	Reduce hemodynamic changes, right ventricular hypertrophy and morphometric changes; suppressed inflammation and oxidative stress	10 mg/kg (*i.p.*)	NA	Han et al. (2016)
Obesity	*In vivo:* C57BL/6J mice. *In vitro:* HepG2 cells and 3T3-L1 adipocytes	*In vivo:* diet-induced obese (DIO) mice. *In vitro:* H_2O_2-induced oxidative stress	Increase the expression of Nrf2, GCLC and CAT, improve glucose metabolism and liver function, decrease body weight gain	*In vivo*: 200 mg/kg/d for 10 weeks (*i.v. In vitro*: 10, 50, and 100 mg/L	NA	Yan et al. (2020)
Skin photoprotective effect	*In vivo* female KM mice	Photoaged mouse model	Prevent UV-induced macroscopic skin lesions, promote the ability of the skin to regain its initial shape, elevated the activities of skin anti-oxidant enzymes, increased skin collagen content, maintained the structural integrity of the skin	50, 100, and 200 l g/mouse following each UV exposure	NA	Kong et al. (2013)
Anti-anaphylactoid activity	*In vivo:*C57BL/6 mice. *In vitro*: Laboratory of allergic disease 2 (LAD2) human mast cells and mouse peritoneal mast cells	a mouse model of hindpaw extravasation	Attenuate calcium flux, decrease degranulation, attenuated degranulation triggered by endogenous and exogenous substances, decrease the activation of the plcγ-pkc-IP3 signaling pathway regulating calcium fluctuations	*In vivo*: 0, 2.5 mg/kg. 5 mg/kg, 10 mg/kg (*i.v.*). *In vitro*: 0, 50 μM, 100 μM, 200 μM. NA	NA	Liu et al. (2014)
Inhibition of hepatic fibrosis	*In vivo*: SD rats	CCl_4-caused fibrogenesis	Decrease in fibrosis, protein expression of *a*-SMA, and MEF-2C gene expression, decreased expression of Tβ-RI, Tβ-RII, MEKK3, MEK5, and phosphorylation of ERk5	5 mg/kg/d for 12 weeks	NA	Zhang et al. (2012)
Type 1 diabetes	*In vivo*: SD rats. *In vitro*: Human epithelial and keratinocytes (HEKs)	*In vivo*: Type 1 diabetes mellitus (T1DM) model	Accelerate diabetic wound healing through promoting angiogenesis and reducing inflammatory response, enhance angiogenesis by upregulation of hypoxia inducible factor-1 alpha (HIF-1a) expression	2/0.4 mg/ml of HSYA/DFO hydrogel solution for five weeks	Deferoxamine (DFO) and HSYA	Gao et al. (2018)
Type 2 diabetes mellitus	*In vivo*: Wistar rats	*In vivo:* HFD feeding-induced T2DM model	Reduce fasting-blood glucose and insulin resistance, up-regulate of PI3K and AKT, inhibit the apoptosis	120 mg/kg (*i.v.*)	NA	Lee et al. (2020)
Polycystic ovary syndrome (PCOS)	*In vivo*: ICR female mice	*In vivo:* Dehydroepiandrosterone-induced PCOS model	Elevate serum E2, P4, LH and AMH levels, reduce FSH. Level, reverse the expression of steroid hormone secretion-related genes Star, hsd3b1, cyp11a1 and cyp19a1, improve GSH content, enhance the activities of antioxidant enzymes SOD, GSH-Px and CAT	3.5 mg/kg (*i. p.*)	HSYA and ginsenoside Rb1	Luo et al. (2020)

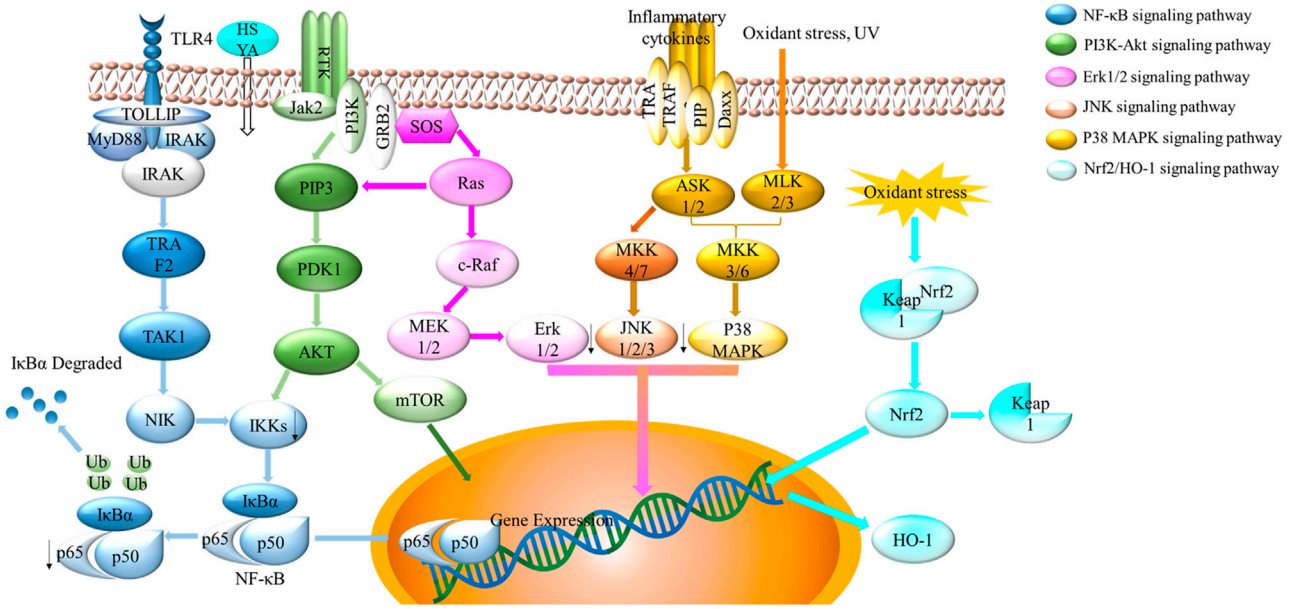

FIGURE 8 | Schematic showing multiple signaling pathways of HSYA. The four crucial signaling pathways were displayed above, including NF-κB signaling pathway, PI3K-Akt signaling pathway, MAPK signaling pathway (Erk1/2, JNK, p38 signaling pathway), and Nrf2/HO-1 signaling pathway.

healthy Chinese female volunteer. The $t_{1/2}$ corresponded to the median of the range from 2.23 to 4.63 h (the average value of 3.17 h) at each dose. But this research had some potential limitations, such as a low-volume sample and only female volunteers, which lack of universality. Moreover, the combination therapy of HSYA and protocatechuic aldehyde greatly promoted the intake of HSYA (Ao et al., 2018).

HYSA is reduced and hydrolyzed, such as hydroxylation, hydroxylation and methylation, dehydration, hydrogenation and hydration, to obtain phase I metabolites under the action of hepatic microsomal drug-metabolizing enzyme in the liver. Phase II metabolism included acetylation and glucuronidation, dehydration, hydrogenation, hydration, hydroxylation with glucuronidation, deglycosylation, methylation and glucuronic acid conjugation reactions (Jin et al., 2016b; Wu et al., 2018). The possible metabolic pathways were summarized in Ahmed and Aljaeid, 2016, **Figure 7**. HSYA and its metabolites are distributed in the heart, liver, spleen, lung, kidney, brain and intestines. In addition, it is almost impossible to cross the healthy blood-brain-barrier (BBB), but easily to penetrate damaged BBB (Sheng et al., 2019).

The low bioavailability of HSYA directly blocks its therapeutic efficiency. It is difficult for HSYA to pass through phospholipid bilayer because of its strong polarity and poor membrane permeability, which is also an important reason for its low bioavailability. Therefore, the design of HSYA delivery systems mainly focused on improving its lipsolubility. Despite, HSYA exists as an undivided molecule in the strong acid environment of the stomach, it cannot be absorbed by the stomach due to its high molecular weight and strong hydrophilicity (Zhang, 2006). Besides, the small intestine actually is the main absorption site of HSYA. However, gastrointestinal metabolism in a weak alkaline environment is not conducive to the absorption of HSYA, on the contrary, it promotes degradation (Wu et al., 2018).

PHARMACOLOGICAL EFFECTS AND MOLECULAR MECHANISM

HSYA shows excellent therapeutic effects on various diseases, such as cardiovascular and cerebrovascular diseases, cancer, and so on. This part provided the biological activity of HSYA in detail (**Table 3**, **Figure 8**).

Cardioprotective Effects

HSYA has been proved to be a superior agent on the cardioprotective system *in vivo* and *in vitro*. HSYA (5 mg/kg, 30 min before ischemia, *i. p.*) was found to improve ischemia/reperfusion (I/R) injury by reducing the releases of cTnI, IL-6. LDH and the myocardial infarction size (Zhou et al., 2019). Similarly, HSYA (4 or 8 mg/kg) could reduce the expression of MIS, CK-MB, and MDA in experimental acute myocardial ischemic model, which induced by left anterior descending coronary artery (LAD) ligation (Tu et al., 2009). Furthermore, HSYA combined with nitroglycerin showed a better therapeutic action on acute myocardial infarction than HSYA alone, which produced a marked increase in SOD, eNOS, and NO content.

The mechanisms of HSYA on cardioprotective effects are related to antioxidant, free radical scavenging abilities, and anti-inflammatory activity. The nuclear factor erythroid 2-related factor 2 (Nrf2) is a transcription factor responsible for the regulation of cellular redox balance and protective antioxidant and phase II detoxification responses in mammals. On basal condition, Nrf2 binding with the chaperon protein Kelch like-ECH-associated

protein 1 (Keap1) located in cytoplasm with inhibition abilities. When facing oxidant stress, Nrf2-Keap1 combination is separated. Nrf2 transports to the nucleus and activates the transcription of genes encoding. Heme oxygenase-1 (HO-1), as one of Nrf2-dependent gene, protects against oxidant stress (Loboda et al., 2016; Reuland et al., 2013). Hu et al. (2016) reported that the combination of HSYA and DSS exerted the markedly antioxidant capacity on increasing the expression of HO-1, the phosphorylation of Akt, and the translocation of Nrf2 (**Figure 8**). Similarly, HSYA attenuated the expression of IL-1β, TNF-α, iNOS, COX-2, MCP-1 on BV2 cells of oxygen and glucose deprivation models (OGD). HSYA also inhibited NF-κB signaling pathway, TLR4 signaling pathway and phosphorylation of p38 (Han et al., 2016; Li et al., 2013). In addition, HSYA decreased the formulation of mitochondrial permeability transition pore in hypoxic cardiac myocytes, thereby inhibiting cardiomyocytes from damage during cardiomyocyte reoxygenation (Huber et al., 2018). In summary, oxidative stress and inflammation related signaling pathways (e.g., Nrf2/OH-1, p38 MAPK, NF-κB signaling pathway and TLR4 signaling pathway all play an important role during the treatment of cardiovascular disease with HSYA.

Neuroprotective Effect

HSYA showed excellent neuroprotective effect. HSYA injection (50 mg/d and 75 mg/d) in patients with acute ischemic stroke of blood stasis syndrome might be to undergo for a phase III clinical trial (Zhu et al., 2020). HSYA (2 mg/kg, tail vein injection) protected the C57BL/6J mice against middle cerebral artery occlusion (MCAO) by decreasing the expression of inflammatory genes factors, including TNF-α, IL-1β, and NO (Lv et al., 2015). HSYA (0.6 mg/100 g, tail vein injection) could also improve spatial learning and memory ability of vascular dementia model rat by promoting angiogenesis and increasing synaptic plasticity (Zhang et al., 2014). Moreover, HSYA (6 mg/kg per day, 2 weeks, *i. v.*) could reduce the accumulation of amyloid precursor protein, improve synaptic function and reverse homocysteine (Hcy) induced cognitive impairment in Alzheimer's disease mice (Lu et al., 2013).

The neuroprotective effect of HSYA might be related to the regulation of TLR4, NF-κB, p-p65, MAPK, PI3K/Akt and Nrf2/HO-1 signaling pathways (Wei et al., 2005; Lv et al., 2015; Deng et al., 2018). NF-κB is a family of dimeric transcription factors central to regulate immune development, immune responses, inflammation, cancer, and other diseases. HSYA inhibited NF-κB to exert neuroprotective effect (Yu et al., 2020). Similarly, HSYA (20 mg/kg for 28 days) could improve motor dysfunction in C57/BL6 mice model of Parkinson by promoting the expression of BDNF, *p*-TrkB/TrkB, DRD3, p-PI3K/PI3K and *p*-AKT/AKT (Wang et al., 2017).

Anticancer Effect

Some studies have found that HSYA exerted anticancer activity in several cancer cells, such as human umbilical vein endothelial cells (HUVEC), HepG2 cells, Skov3 cells, as well as some *in vivo* studies. HSYA could eliminate reactive oxygen species (ROS), prevent apoptosis from membrane permeability, and inhibit proliferation and migration (Ma et al., 2019a; Chen et al., 2019; Zhang et al., 2019). HSYA also increased the thymus index, and effectively down-regulate the mRNA levels of forkhead box P3-positive (Foxp3) and retinoic acid receptor-related orphan receptor-gamma-t ($ROR\gamma t$), which contributed to improve the tumor immune microenvironment-the key points of tumor cell proliferation and invasion (Ma et al., 2019b). What is particularly noteworthy is the anticancer abilities of HSYA might related to the excellent antioxidant effect.

Anticoagulant Effect

PAF, as the most effective platelet activator known so far, has a wide range of biological activities, and can be synthesized by a variety of cells such as platelets, leukocytes, endothelial cells. Anticoagulant effect of HSYA plays a significant mediating role in many pathological processes, such as tissue IR injury, coronary heart disease, atherosclerosis, cerebrovascular disease and many other cardiovascular diseases. HSYA dose-dependently inhibited the specific binding between [^{3}H] PAF and washed rabbit platelet, which is considered as a new generation PAF receptor antagonist in the future (Zang et al., 2002). PAF-activated human small airway epithelial cells model was pretreated with HSYA. Guo et al. (2018) proposed that HSYA could attenuate the PAF-induced inflammatory factors, destruct cell-barrier function, and inhibit the expression of protein kinase C, MAPK, activator protein-1, and NF-κB activation to show anticoagulant effect.

Other Pharmacological Effects

In addition to the biological activities discussed above, HSYA also has other diverse pharmacological effects, such as immunodeficiency, anaphylactoid, hepatic fibrosis, pulmonary arterial hypertension, skin photosensitivity, Type 1 diabetes, vascular dementia, and so on.

HSYA is an immunomodulator that regulates the inflammatory response induced by lipopolysaccharide in various cells, including human non-small lung cancer cell line (A549 cells), H1299 and Eahy926 human endothelium cells. It could inhibit many kinase activities related to inflammatory factors, such as TNFα, IL-1β, and IL-6. HSYA could also inhibit the pro-inflammatory proteins expression, such as NF-κB p65, PI3K/Akt/mTOR, MAPK TLR-4, Myd88 and ICAM-1 (Han and Zhao, 2010; Jin et al., 2016; Jiang et al., 2019. HSYA was also proved to relieve certain respiratory conditions by decreasing mRNA levels of ICAM-1 and E-selectin elevation (Liu et al., 2014; Zhang et al., 2017). Moreover, another study implemented by Zheng et al. (2019) showed that HSYA could attenuate ovalbumin-induced allergic asthma in guinea pigs.

HSYA possesses a strong vascular relaxation effect on pulmonary arterial hypertension (PAH). It reduced the vascular tension by activating the Kv channel in pulmonary vascular smooth muscle cells (PVSMCs) (Bai et al., 2012). HSYA (6 mg/kg for 11 days) promoted angiogenesis in ischemic mice. The therapeutic mechanisms of HSYA might be associated to significantly increase the capillary-like tube formation and migration of HUVEC, enhance the expression of angiopoietin 1 and Tie-2, phosphorylations of Tie2, Akt and extracellular signal-regulated kinase 1/2 (Chen T. et al., 2016).

It is also reported that HSYA could exert protection on macroscopic skin lesions induced by ultraviolet rays (UV). It could promote the skin to regain its initial shape, elevate the activities of skin anti-oxidant enzymes, increase skin collagen content and maintain the structural integrity of the skin (Kong et al., 2013).

The combination of HSYA and deferoxamine (DFO) was discovered to improve type 1 diabetes by accelerating diabetic wound healing, promoting angiogenesis, reducing the inflammatory response, and up-regulating the expression of hypoxia-inducible factor-1 *a* (HIF-1 α) (Gao et al., 2018).

DISCUSSION AND CONCLUSION

In the present review, we systematically summarized the materials about HSYA, including acquisition methods, extraction and detection methods, pharmacokinetics, pharmacological effects and molecular mechanism. HSYA is proved to be an excellent antioxidant, anti-inflammatory and anticoagulant agent, so it plays an exceptional role in the treatment of cardiovascular and cerebrovascular diseases by down-regulating NF-κB signaling pathways, inhibiting MAPK signaling pathways, and attenuating the activation of Nrf-2/HO-1 signaling pathways. However, it is easily to degrade in the process of storage, extraction and separation procedure due to its chemical instability, which brings great challenges to the application of HSYA. Another major challenge is the low bioavailability caused by strong polarity. A large number of studies have been carried out to improve the chemical instability and bioavailability. Microemulsions, self-emulsifying systems, nanoparticles and other drug delivery systems have gradually improved the bioavailability, chemical stability, cellular uptake and biological activity of HSYA, which will be evaluated in clinical trials later.

Although great progress has been made in the research and application of HSYA in the past few decades, there are still many problems and challenges. First of all, chemical instability and low bioavailability of HSYA are still far from being resolved, which is still a key issue of the future research. It is important to continue the development of viable drug delivery systems for HSYA. The crucial aspects will involve in the enhancement of the solubility and bioavailability, as well as methods for selectively targeting these delivery systems to disease sites. Secondly, HSYA has been used to treat cardiovascular and cerebrovascular diseases clinically in China, but the drug target has not been completely revealed at present, which needs in-depth study later. Finally, the approach of obtaining HSYA from plants is cumbersome and complicated, and the yield is unsatisfactory. Chemical synthesis might pollute the environment, so it does not recommend to popularize. Biosynthesis is characterized by high efficiency, energy saving, and environmental protection, and it will transform into the major source of HSYA in the near future.

In short, it is the first time to systematically summarize the basic information about HSYA, which might provide relatively comprehensive basic data for the related research of HSYA.

AUTHOR CONTRIBUTIONS

HX, FZ and PW performed the frame design of the manuscript. FZ collected the data and drafted the manuscript. YJ, XZ and DC helped to organize the data. PW revised the manuscript. All authors read and approved the final manuscript.

FUNDING

This work was supported by grants from National Key Research and Development Program of China (2017YFC1702104, 2017YFC1702303), the National Natural Science Foundation of China (81830111, 81774201), National Science and Technology Major Project of China (2019ZX09201005-001-003), the Youth Innovation Team of Shaanxi Universities and Shaanxi Provincial Science and Technology Department Project (2016SF-378), the Fundamental Research Funds for the Central public welfare research institutes (ZXKT17058). Natural Science Foundation of Shandong Province (ZR2019ZD24, ZR2019YQ30).

The funding agencies had no role in the study design, the collection, analysis, or interpretation of data, the writing of the report, or the decision to submit the article for publication.

REFERENCES

Ahmed, T., and Aljaeid, B. (2016). Preparation, characterization, and potential application of chitosan, chitosan derivatives, and chitosan metal nanoparticles in pharmaceutical drug delivery. *Ddt* 10, 483–507. doi:10.2147/DDDT.S99651

Ao, H., Feng, W., and Peng, C. (2018). Hydroxysafflor yellow A: a promising therapeutic agent for a broad spectrum of diseases. *Evid. base Compl. Alternative Med.* 2018, 1–17. doi:10.1155/2018/8259280

Bacchetti, T., Morresi, C., Bellachioma, L., and Ferretti, G. (2020). Antioxidant and pro-oxidant properties of carthamus tinctorius, hydroxy safflor yellow A, and safflor yellow A. *Antioxidants* 9, 119. doi:10.3390/antiox9020119

Bie, X. D., Han, J., and Dai, H. B. (2010). Effects of hydroxysafflor yellow A on the experimental traumatic brain injury in rats. *J. Asian. Nat. Prod. Res.* 12, 239–247. doi:10.1080/10286020903510636

Bai, Y., Lu, P., Yu, C., Chen, M., He, F., et al. (2012). Hydroxysafflor yellow A (HSYA) from flowers of Carthamus tinctorius L. and its vasodilatation effects on pulmonary artery. *Molecules* 17, 14918–14927. doi:10.3390/molecules171214918

Cao, H. Y., Qin, X. D., Liu, C., Zhao, X. Z., Ma, Y. H., Zhou, J. N., et al. (2020). Establishment of fluorescence sensitization method for Hydroxysafflor yellow A. *Evid. Based. Complement. Alternat, Med.* 2020 (1–13), 3027843. doi:10.1155/2020/3027843

Chen, S., Ma, J., Zhu, H., Deng, S., Gu, M., and Qu, S. (2019). Hydroxysafflor yellow A attenuates high glucose-induced human umbilical vein endothelial cell dysfunction. *Hum. Exp. Toxicol.* 38, 685–693. doi:10.1177/0960327119831065

Chen, X., Wang, Y., Zhang, L., and Gao, Y. (2020a). Hydroxysafflor yellow A of carthamus tinctorius L., represses the malignant development of esophageal cancer cells via regulating NF-κB signaling pathway. *Cell Biochem. Biophys.* 78, 511. doi:10.1007/s12013-020-00934-1

Chen, Y., Li, Y., Chen, X., Wang, L., Sun, C., Yan, W., et al. (2010). Development and validation of a HPLC method for the determination of five bioactive

compounds in the "Xuebijing" injection. *Anal. Lett.* 43, 2456–2464. doi:10.1080/00032711003698739

Chen, T., Chen, N., Pang, N., Xiao, L., Li, Y., Li, R., et al. (2016a). Hydroxysafflor yellow A promotes angiogenesis via the angiopoietin 1/tie-2 signaling pathway. *J. Vasc. Res.* 53, 245–254. doi:10.1159/000452408

Chen, C. P., Pei, J., Wu, Y. Y., Ren, C. X., Chen, J., Liu, W., et al. (2016b). [Cloning,Bioinformatic analysis of chalcone-flavonone isomerase gene(CHI) and relationship between expression of CHI and accumulation of HSYA in Carthamus tinctorius]. *Zhong Yao Cai* 39, 499–503.

Collins, D. R. J., Tompson, A. C., Onakpoya, I. J., Roberts, N., Ward, A. M., and Heneghan, C. J. (2017). Global cardiovascular risk assessment in the primary prevention of cardiovascular disease in adults: systematic review of systematic reviews. *BMJ Open.* 7 (1–13), e013650. doi:10.1136/bmjopen-2016-013650

Chu, D., Liu, W., Huang, Z., Liu, S., Fu, X., and Liu, K. (2006). Pharmacokinetics and excretion of hydroxysafflor yellow A, a potent neuroprotective agent from safflower, in rats and dogs. *Planta Med.* 72, 418–423. doi:10.1055/s-2005-916249

Dai, Y., and Ge, J. (2012). Clinical use of aspirin in treatment and prevention of cardiovascular disease. *Thrombosis* [Epub ahead of print]. doi:10.1109/cis.2012.56

Deng, L., Wan, H., Zhou, H., Yu, L., and He, Y. (2018). Protective effect of hydroxysafflor yellow A alone or in combination with acetylglutamine on cerebral ischemia reperfusion injury in rat: a PET study using 18F-fuorodeoxyglucose. *Eur. J. Pharmacol.* 825, 119–132. doi:10.1016/j.ejphar.2018.02.011

Desborough, M. J. R., and Keeling, D. M. (2017). The aspirin story–from willow to wonder drug. *Br. J. Haematol.* 177, 674–683. doi:10.1111/bjh.14520

Donahue, M. J., and Hendrikse, J. (2018). Improved detection of cerebrovascular disease processes: introduction to the journal of cerebral blood flow and metabolism special issue on cerebrovascular disease. *J. Cerebr. Blood Flow Metabol.* 38, 1387–1390. doi:10.1177/0271678X17739802

Eichhorn, E. J., and Gheorghiade, M. (2002). Digoxin. *Prog. Cardiovasc. Dis.* 44, 251–266. doi:10.1053/pcad.2002.31591

Fan, L., Pu, R., Zhao, H. Y., Liu, X., Ma, C., Wang, B. R., et al. (2011). Stability and degradation of hydroxysafflor yellow A and anhydrosafflor yellow B in the Safflower injection studied by HPLC-DAD-ESI-MSn. *J. Chin. Pharmaceut. Sci.* 20, 47–56. doi:1-47-1010.5246/jcps.2011.01.007

Gao, S.-Q., Chang, C., Li, J.-J., Li, Y., Niu, X.-Q., Zhang, D.-P., et al. (2018). Co-delivery of deferoxamine and hydroxysafflor yellow a to accelerate diabetic wound healing via enhanced angiogenesis. *Drug Deliv.* 25, 1779–1789. doi:10.1080/10717544.2018.1513608

Ghasemiyeh, P., and Mohammadi-Samani, S. (2018). Solid lipid nanoparticles and nanostructured lipid carriers as novel drug delivery systems: applications, advantages and disadvantages. *Res. Pharm. Sci.* 13, 288–303. doi:10.4103/1735-5362.235156

Guo, L. F., Zhang, Y., Hu, Z. H., Hu, X. L., Xu, N. S., Zhang, X. S., et al. (2013). Clustering analysis of safflower (*Carthamuss tinctorius* L.) germplasm resources based on morphological markers. *J. Henan Agric. Sci.* 42, 41–97. doi:10.15933/j.cnki.1004-3268.2013.02.020

Guo, X., Zheng, M., Pan, R., Zang, B., and Jin, M. (2018). Hydroxysafflor yellow a suppresses platelet activating factor-induced activation of human small airway epithelial cells. *Front. Pharmacol.* 9, 859–870. doi:10.3389/fphar.2018.00859

Han, B., and Zhao, H. (2010). Effects of hydroxysafflor yellow a in the attenuation of MPTP neurotoxicity in mice. *Neurochem. Res.* 35, 107–113. doi:10.1007/s11064-009-0035-4

Han, D., Wei, J., Zhang, R., Ma, W., Shen, C., Feng, Y., et al. (2016). Hydroxysafflor yellow a alleviates myocardial ischemia/reperfusion in hyperlipidemic animals through the suppression of TLR4 signaling. *Sci. Rep.* 6, 35319–35332. doi:10.1038/srep35319

Heller, W., and Hahlbrock, K. (1980). Highly purified "flavanone synthase" from parsley catalyzes the formation of naringenin chalcone. *Arch. Biochem. Biophys.* 200, 617–619. doi:10.1016/0003-9861(80)90395-1

Hong, B., Wang, Z., Xu, T., Li, C., and Li, W. (2015). Matrix solid-phase dispersion extraction followed by high performance liquid chromatography-diode array detection and ultra performance liquid chromatography-quadrupole-time of flight-mass spectrometer method for the determination of the main compounds from *Carthamus tinctorius* L. (Hong-hua). *J. Pharmaceut. Biomed. Anal.* 107, 464–472. doi:10.1016/j.jpba.2015.01.040

Hong, S.-C., Yoo, S.-Y., Kim, H., and Lee, J. (2017). Chitosan-based multifunctional platforms for local delivery of therapeutics. *Mar. Drugs* 15 (1–16), 60. doi:10.3390/md15030060

Hu, T., Wei, G., Xi, M., Yan, J., Wu, X., Wang, Y., et al. (2016). Synergistic cardioprotective effects of danshensu and hydroxysafflor yellow a against myocardial ischemia-reperfusion injury are mediated through the Akt/Nrf2/HO-1 pathway. *Int. J. Mol. Med.* 38, 83–94. doi:10.3892/ijmm.2016.2584

Huber, G., Priest, S., and Geisbuhler, T. (2018). Cardioprotective effect of hydroxysafflor yellow A via the cardiac permeability transition pore. *Planta. Med.* 84, 507–518. doi:10.1055/s-0043-122501

Jiang, M., Zhou, L. Y., Xu, N., and An, Q. (2019). Hydroxysafflor yellow A inhibited lipopolysaccharide-induced non-small cell lung cancer cell proliferation, migration, and invasion by suppressing the PI3K/AKT/mTOR and ERK/MAPK signaling pathways. *Thorac. Cancer* 10, 1319–1333. doi:10.1111/1759-7714.13019

Jin, M., Sun, C.-y., and Zang, B.-x. (2016a). Hydroxysafflor yellow A attenuate lipopolysaccharide-induced endothelium inflammatory injury. *Chin. J. Integr. Med.* 22, 36–41. doi:10.1007/s11655-015-1976-x

Jin, Y., Wu, L., Tang, Y., Cao, Y., Li, S., Shen, J., et al. (2016b). UFLC-Q-TOF/MS based screening and identification of the metabolites in plasma, bile, urine and feces of normal and blood stasis rats after oral administration of hydroxysafflor yellow A. *J. Chromatogr. B* 1012–1013, 124–129. doi:10.1016/j.jchromb.2016.01.023

Knogge, W., Schmelzer, E., and Weissenböck, G. (1986). The role of chalcone synthase in the regulation of flavonoid biosynthesis in developing oat primary leaves. *Arch. Biochem. Biophys.* 250, 364–372. doi:10.1016/0003-9861(86)90738-1

Koga, K., Takarada, N., and Takada, K. (2010). Nano-sized water-in-oil-in-water emulsion enhances intestinal absorption of calcein, a high solubility and low permeability compound. *Eur. J. Pharm. Biopharm.* 74, 223–232. doi:10.1016/j.ejpb.2009.09.004

Kong, S.-Z., Shi, X.-G., Feng, X.-X., Li, W.-J., Liu, W.-H., Chen, Z.-W., et al. (2013). Inhibitory effect of hydroxysafflor yellow A on mouse skin photoaging induced by ultraviolet irradiation. *Rejuvenation Res.* 16, 404–413. doi:10.1089/rej.2013.1433

Lee, M., Li, H., Zhao, H., Suo, M., and Liu, D. (2020). Effects of Hydroxysafflor Yellow A on the PI3K/AKT pathway and apoptosis of pancreatic β-Cells in Type 2 diabetes mellitus rats. *Diabetes. Metab. Syndr. Obes* 13, 1097–1107. doi:10.2147/DMSO.S246381

Lee, S.-E., Lee, J.-K., Jang, W.-S., Kim, T.-H., Tunsirikongkon, A., Choi, J.-S., et al. (2016). Enhancement of stability and controlled drug release of lipid nanoparticles by modified solvent-evaporation method. *Colloid. Surface. Physicochem. Eng. Aspect.* 508, 294–300. doi:10.1016/j.actbio.2014.07.032

Li, Y., Zhang, Z., and Zhang, J. (2007). Determination of hydroxysafflor yellow A in rat plasma and tissues by high-performance liquid chromatography after oral administration of safflower extract or safflor yellow. *Biomed. Chromatogr.* 21, 326–334. doi:10.1002/bmc.769

Li, H., Huang, L., Ping, Q., and Zhao, H. (2009). Study on the stability of safflower yellow. *Strait. Pharm. J.* 21, 12–14.

Li, J. R., Sun, M. J., Ping, Q. N., Chen, X. J., Qi, J. P., and Han, D. E. (2010a). Metabolism, excretion and bioavailability of hydroxysafflor yellow A after oral administration of its lipid-based formulation and aqueous solution in rats. *Chin. J. Nat. Med.* 8, 233–240. doi:10.3724/SP.J.1009.2010.00233

Li, S., Kesarla, R., and Omri, A. (2013). Formulation strategies to improve the bioavailability of poorly absorbed drugs with special emphasis on self-emulsifying systems. *ISRN Pharmaceut.* 2013 (1–16), 1. doi:10.1155/2013/848043

Li, L., Yang, Y., Hou, X., Gu, D., Ba, H., Abdulla, R., et al. (2013a). Bioassay-guided separation and purification of water-soluble antioxidants from *Carthamus tinctorius* L. by combination of chromatographic techniques. *Separ. Purif. Technol.* 104, 200–207. doi:10.1016/j.seppur.2012.11.027

Li, J., Zhang, S. Y., Lu, M. R., Chen, Z. B., Chen, C., Han, L. J., et al. (2013b). Hydroxysafflor yellow A suppresses inflammatory responses of BV2 microglia after oxygen–glucose deprivation. *Neurosci. Lett.* 535, 51–56. doi:10.1016/j.neulet.2012.12.056

Li, C. Y., Chu, J. H., Zhang, J., Dai, G. L., Zou, J. D., and Ju, W. Z. (2014). Determination of hydroxysafflor yellow A in human plasma by LC-MS/MS analysis. *Chin. Pharmacol. Bull.*, 1402–1407. doi:10.3969/j.issn.1001-1978.2014.10.016

Li, L. J., Jiang, T. T., and Guo, J. (2016). Preparation of HSYA by organic reagent method. *Strait. Pharm. J.* 28, 30–34.

Li, Y., Wang, Z., Chang, H., Wang, Y., and Guo, M. (2010b). Expression of CT-wpr, screened by cDNA-AFLP approach, associated with hydroxysafflor yellow A in *Carthamus tinctorius* L. *Biochem. Systemat. Ecol.* 38, 1148–1155. doi:10.1016/j.bse.2010.10.010

Li, X., Huang, L., and Fu, Z. (2011). The influence of light on stability of Safflowler Yellow. *Strait. Pharm. J.* 23, 64–66.

Liang, H. Z., Dong, W., Yu, Y. L., Yang, H. Q., Xu, L. J., and Niu, Y. G. (2015). Advances in studies on safflower (*carthamus tinctorius* L.) at home and abroad. *J. Anhui Agri. Sci.* 43, 71–74. doi:10.13989/j.cnki.0517-6611.2015.16.030

Liu, Y. L., Liu, Y. J., Liu, Y., Li, X. S., Liu, S. H., Pan, Y. G., et al. (2014). Hydroxysafflor yellow A ameliorates lipopolysaccharide-induced acute lung injury in mice via modulating toll-like receptor 4 signaling pathways. *Int. Immunopharm.* 23, 649–657. doi:10.1016/j.intimp.2014.10.018

Liu, Z., Liu, L., Liu, Y., Wang, S., Zhang, S., Dong, R., et al. (2020). Hydroxysafflor yellow A induces autophagy in human liver cancer cells by regulating Beclin 1 and ERK expression. *Exp Ther Med.* 9, 2989–2996. doi:10.3892/etm.2020.8552

Loboda, A., Damulewicz, M., Pyza, E., Jozkowicz, A., and Dulak, J. (2016). Role of Nrf2/HO-1 system in development, oxidative stress response and diseases: an evolutionarily conserved mechanism. *Cell. Mol. Life Sci.* 73, 3221–3247. doi:10.1007/s00018-016-2223-0

Lopes, L. B. (2014). Overcoming the cutaneous barrier with microemulsions. *Pharmaceutics* 28, 52–77. doi:10.3390/pharmaceutics6010052

Lu, Y. Q., Luo, Y., He, Z. F., Chen, J., Yan, B., Wang, Y., et al. (2013). Hydroxysafflor yellow A ameliorates homocysteine-induced Alzheimer-like pathologic dysfunction and memory/synaptic disorder. *Rejuvenation Res.* 16, 446–452. doi:10.1089/rej.2013.1451

Luo, M., Huang, J. C., Yang, Z. Q., Wang, Y. S., Guo, B., and Yue, Z. P. (2020). Hydroxysafflor yellow A exerts beneficial effects by restoring hormone secretion and alleviating oxidative stress in polycystic ovary syndrome mice. *Exp. Physiol.* 105, 282–292. doi:10.1113/EP088147

Lv, X. Y., Mo, J. Q., Jiang, T., Zhong, F. R., Jia, Z. H., Li, J. W., et al. (2011). Novel multilayered porous silicon-based immunosensor for determining Hydroxysafflor yellow A. *Appl. Surf. Sci.* 257, 1906–1910. doi:10.1016/j.apsusc.2010.09.024

Lv, L. Z., Tong, C. Q., Lv, Q., Tang, X. J., Li, L. M., Fang, Q. X., et al. (2012). Enhanced absorption of hydroxysafflor yellow A using a self-double-emulsifying drug delivery system: *in vitro* and *in vivo* studies. *Int. J. Nanomed.* 7, 4099–4107. doi:10.2147/IJN.S33398

Lv, Y., Qian, Y., Fu, L., Chen, X., Zhong, H., and Wei, X. (2015). Hydroxysafflor yellow A exerts neuroprotective effects in cerebral ischemia reperfusion-injured mice by suppressing the innate immune TLR4-inducing pathway. *Eur. J. Pharmacol.* 769, 324–332. doi:10.1016/j.ejphar.2015.11.036

Lv, X., Zhang, S. G., Ma, H. P., Dong, P. P., Ma, X. D., Xu, M., et al. (2018). *In situ* monitoring of the structural change of microemulsions in simulated gastrointestinal conditions by SAXS and FRET. *Acta Pharm. Sin. B.* 8, 655–665. doi:10.1016/j.apsb.2018.05.008

Ma, G. N., Yu, F. L., Zhang, H., Li, Z. P., and Mei, X. G. (2014). Pharmacokinetics and biopharmaceutics of hydroxysafflor yellow A: research advances. *J. Int. Pharm. Res.* 41, 195–199. doi:10.13220/j.cnki.jipr.2014.02.012.220

Ma, Y., Feng, C., Wang, J., Chen, Z., Wei, P., Fan, A. R., et al. (2019a). Hydroxyl safflower yellow A regulates the tumor immune microenvironment to produce an anticancer effect in a mouse model of hepatocellular carcinoma. *Oncol. Lett.* 17, 3503–3510. doi:10.3892/ol.2019.9946

Ma, Y. C., Li, M. M., Wu, Q., Xu, W. F., Lin, S., Chen, Z. W., et al. (2019b). Hydroxysafflor yellow A sensitizes ovarian cancer cells to chemotherapeutic agent by decreasing WSB1 expression. *Eur. J. Integr. Med.* 25, 6–12. doi:10.1016/j.eujim.2018.11.007

Meselhy, M. R., Kadota, S., Momose, Y., Hatakeyama, N., Kusai, A., Hattori, M., et al. (1993). Two new quinochalcone yellow pigments from Carthamus tinctorius and Ca^{2+} antagonistic activity of tinctormine. *Chem. Pharm. Bull.* 41, 1796–1802. doi:10.1248/cpb.41.1796

Min, F., Sun, H., Wang, B., Ahmad, N., Guo, H., Gao, H. T., et al. (2020). Hepatoprotective effects of hydroxysafflor yellow A in D-galactose-treated aging mice. *Eur. J. Pharmacol.* 881 (1–36), 173214. doi:10.1016/j.ejphar.2020.173214

Pang, B., Zheng, Q. F., and Liu, W. (2015). Synthetic biology in natural medicine research. *Scientia. Sinica. Vitae.* 45, 1015–1026. doi:10.1360/N052015-00041

Pan, Y., Zheng, D. Y., Liu, S. M., Meng, Y., Xu, H. Y., Zhang, Q., et al. (2012). Hydroxysafflor yellow A attenuates lymphostatic encephalopathy-induced brain injury in rats. *Phytother. Res* 26, 1500–1506. doi:10.1002/ptr.4594

Pu, W., Zhang, H., Wang, M., Liu, Y. N., Sun, L. L., and Ren, X. L. (2017). Superior stability of Hydroxysafflor Yellow A in Xuebijing injection and the associated mechanism. *Molecules* 22 (1–12), 2129. doi:10.3390/molecules22122129

Qi, J., Jin, X., Huang, L., and Ping, Q. (2007). Simultaneous determination of hydroxysafflor yellow A and ferulic acid in rat plasma after oral administration of the co-extractum of *Rhizoma* chuanxiong and *Flos Carthami* by HPLC–diode array detector. *Biomed. Chromatogr.* 21, 816–822. doi:10.1002/bmc.821

Qi, J., Zhuang, J., Wu, W., Lu, Y., Song, Y. M., Zhang, Z. T., et al. (2011). Enhanced effect and mechanism of water-in-oil microemulsion as an oral delivery system of hydroxysafflor yellow A. *Int. J. Nanomed.* 6, 985–991. doi:10.2147/IJN.S18821

Reuland, D. J., McCord, J. M., and Hamilton, K. L. (2013). The role of Nrf2 in the attenuation of cardiovascular disease. *Exerc. Sport Sci. Rev.* 41, 162–168. doi:10.1097/JES.0b013e3182948a1e

Sheng, C., Peng, W., Xia, Z., and Wang, Y. (2019). Plasma and cerebrospinal fluid pharmacokinetics of hydroxysafflor yellow A in patients with traumatic brain injury after intravenous administration of Xuebijing using LC-MS/MS method. *Xenobiotica* 50, 545–551. doi:10.1080/00498254.2019.1668983

Sun, M. J., Chen, X. J., and Ping, Q. N. (2009). HPLC analysis of the hydroxysafflor yellow A in excretion of rat. *Pharm. Clin. Res.* 17, 191–194.

Sun, X., Wei, X., Qu, S., Zhao, Y., and Zhang, X. (2010). Hydroxysafflor Yellow A suppresses thrombin generation and inflammatory responses following focal cerebral ischemia–reperfusion in rats. *Bioorg. Med. Chem. Lett.* 20, 4120–4124. doi:10.1016/j.bmcl.2010.05.076

Sun, Y. W., He, Y., Zhang, R. P., Huang, J. W., and Gu, M. C. (2013). Optimization of ultrasonic extraction conditions of safflower yellow from *Carthamus tinctorius* by response surface methodology. *J. Chin. Med. Mater.* 36, 2018–2022. doi:10.13863/j.issn1001-4454.2013.12.001

Suzuki, T., Ishida, M., Kumazawa, T., and Sato, S. (2017). Oxidation of 3, 5-di-C-(per-O-acetylglucopyranosyl) phloroacetophenone in the synthesis of hydroxysafflor yellow A. *Carbohydr. Res.* 448, 52–56. doi:10.1016/j.carres.2017.05.009

Tan, L., Wang, Y., Jiang, Y., Wang, R., Zu, J., and Tan, R. (2020). Hydroxysafflor Yellow A together with blood-brain barrier regulator Lexiscan for cerebral ischemia reperfusion injury treatment. *ACS Omega* 5, 19151–19164. doi:10.1021/acsomega.0c02502

Tang, J., Lou, Z., Wang, Y., and Guo, M. (2010). Expression of a small heat shock protein (CTL–hsyapr) screened by cDNA-AFLP approach is correlated with hydroxysafflor yellow A in safflower (*Carthamus tinctorius* L.). *Biochem. Systemat. Ecol.* 38, 722–730. doi:10.1016/j.bse.2010.06.001

Tapeinos, C., Battaglini, M., and Ciofani, G. (2017). Advances in the design of solid lipid nanoparticles and nanostructured lipid carriers for targeting brain diseases. *J. Contr. Release* 264, 306–332. doi:10.1016/j.jconrel.2017.08.033

Tian, L., Wu, G. R., and Wang, Y. (2007). Quality assessment of *Carthamus tinctorius* L. In emin country, tacheng prefecture, xinjiang. *China. Pharmaceuticals* 16, 5–7.

Tong, W., Sun, P., Yang, X., Huang, L. L., and Hu, S. Q. (2011). Study on relativity of safflower color and hydroxysafflor yellow A. *South west China. J. Agric. Sci.* 24, 101–104. doi:10.16213/j.cnki.scjas.2011.01.035

Tu, Y. H., Xue, Y. R., Guo, D. D., Sun, L. N., and Guo, M. L. (2009). Hydroxysafflor yellow A reduces myocardial infarction size after coronary artery ligation in rats. *Pharm. Biol.* 47, 458–462. doi:10.1080/13880200902822612

Wang, S., Sun, M., and Ping, Q. (2008). Enhancing effect of labrafac lipophile WL 1349 on oral bioavailability of hydroxysafflor yellow A in rats. *Int. J. Pharm. (Amst.)* 358, 198–204. doi:10.1016/j.ijpharm.2008.03.006

Wang, G., Li, Q. Y., Fang, Q. L., Han, M., and Gao, J. Q. (2009). Uptake and transport of hydroxysafflor yellow A in Caco-2 cells monolayer. *J. Chin. Pharmaceut. Sci.* 44, 353–357.

Wang, H. (2017). *Studies on the extraction and purification and stability of HSYA*. Shanxi, China: Shanxi university.

Wang, J., Wang, J., Wang, X., Liu, L., Hu, J. H., and Yu, X. (2016). Molecular mechanism of inhibition of the abnormal proliferation of human umbilical vein endothelial cells by Hydroxysafflor-yellow A. *Pharm. Biol.* 54, 1800–1807. doi:10.3109/13880209.2015.1129541

Wang, J. P., Wang, P., Gui, S. Q., Li, Y., Chen, R. H., Zeng, R. Q., et al. (2017). Hydroxysafflor yellow A improves motor dysfunction in the rotenone-induced mice model of Parkinson's disease. *Front. Pharmacol.* 8 (1–10), 613. doi:10.1007/s11064-017-2176-1

Wang, N., He, D., Zhou, Y., Wen, J., Liu, X. Q., Li, P, Y., et al. (2019). Hydroxysafflor yellow A actives BKCa channels and inhibits L-type Ca channels to induce vascular relaxation. *Eur. J. Pharmacol.* 870 (1–10), 172873. doi:10.1016/j.ejphar.2019.172873

Wang, Y., Du, S. Y., Wu, Q., Xiao, Y., Wu, H. C., Lu, X. J., et al. (2012). Optimization of smashing tissue extraction of hydroxyl safflor yellow A

from *carthamus tinctorius* L. *Lishizhen Med. Materia. Med. Res.* 9, 2144–2145. doi:10.3969/j.issn.1008-0805.2012.09.013

Wei, X. B., Liu, H. Q., Sun, X., Fu, F. H., Zhang, X. M., Wang, J., et al. (2005). Hydroxysafflor yellow A protects rat brains against ischemia-reperfusion injury by antioxidant action. *Neurosci. Lett.* 386, 58–62. doi:10.1016/j.neulet.2005.05.069

Wen, A. D., Yang, J., Jia, Y. Y., Yang, Z. F., Tian, Y., Wu, Y., et al. (2008). A rapid and sensitive liquid chromatography–tandem mass spectrometry (LC–MS/MS) method for the determination of hydroxysafflor yellow A in human plasma: application to a pharmacokinetic study. *J. Chromatogr. B.* 876, 41–46. doi:10.1016/j.jchromb.2008.10.007

Wu, L., Tang, Y., Shan, C., Chai, C., Zhou, Z., Shi, X. Q., et al. (2018). A comprehensive *in vitro* and *in vivo* metabolism study of hydroxysafflor yellow A. *J. Mass Spectrom.* 53, 99–108. doi:10.1002/jms.4041

Wu, Y., Wang, L., Jin, M., and Zang, B. (2012). Hydroxysafflor yellow A alleviates early inflammatory response of bleomycin-induced mice lung injury. *Biol. Pharm. Bull.* 35, 515–522. doi:10.1248/bpb.35.515

Xiong, Q. M., Min, C., Liu, Y., Pan, M. F., and Liu, Q. H. (2004). Pharmacokinetics of hydroxysafflor yellow A. *Chin. J. Pharm.* 35, 228–230.

Xu, L. J., Liang, H. Z., Yu, Y. L., Tan, Z. W., Yang, H. Q., Dong, W., et al. (2018). *Carthamus tinctorius* L.: evaluation on correlations of hydroxysafflor with flower color and the difference among cultivars. *Chin. Agricu. Sci. Bull.* 34, 41–45.

Yan, K., Wang, X., Pan, H., Wang, L. J., Yang, H. B., Liu, M. J., et al. (2020). Safflower Yellow and its main component HSYA alleviate diet-induced obesity in mice: possible involvement of the increased antioxidant enzymes in liver and adipose tissue. *Front. Pharmacol.* 11 (1–13), 482. doi:10.3389/fphar.2020.00482

Yang, J., Wang, Y., and Guo, M. L. (2011). Identification and mapping of a novel hydroxysafflor yellow A (HSYA) biosynthetic gene in *Carthamus Tinctorius*. *Biochem. Genet.* 49, 410–415. doi:10.1007/s10528-011-9417-9

Yang, Y., Dai, F., Liu, S., and Kuang, C. (2008). Study on extraction technology of yellow pigment from *Carthamus tinctorius* with microwave extraction. *Food Res. Dev.* 29, 190–192.

Yang, X., Chen, L., Li, Y., Gao, F., Yan, Z., Zhang, P., et al. (2020a). Protective effect of Hydroxysafor Yellow A on cerebral ischemia reperfusion-injury by regulating GSK3β-mediated pathways. *Neurosci. Lett.* 736 (1–25), 135258. doi:10.1016/j.neulet.2020.135258

Yang, X., Li, Y., Chen, L., Xu, M. G., Wu, J. B., Zhang, P., et al. (2020b). Protective effect of hydroxysafflor yellow A on dopaminergic neurons against 6-hydroxydopamine, activating anti-apoptotic and anti-neuroinflammatory pathways. *Pharm. Biol.* 58 (1), 686–694. doi:10.1080/13880209.2020.1784237

Yang, Z., Yang, J., Jia, Y., Tian, Y., and Wen, A. (2009). Pharmacokinetic properties of hydroxysafflor yellow A in healthy Chinese female volunteers. *J. Ethnopharmacol.* 124, 635–638. doi:10.1016/j.jep.2009.02.026

Ye, J. X., Wang, M., Wang, R. Y., Liu, H. T., Qi, Y. D., Fu, J. H., et al. (2020). Hydroxysafflor yellow A inhibits hypoxia/reoxygenation-induced cardiomyocyte injury via regulating the AMPK/NLRP3 inflammasome pathway [published online ahead of print, 2020 Feb 19]. *Int. Immunopharm.* 82 (1–7), 106316. doi:10.1016/j.intimp.2020.106316

Yue, M., Zang, B. X., Li, J. R., and Wang, J. F. (2003). Preliminary study on the thermal stability of hydroxysafflor yellow A. *China J. Chin. Mater. Med.* 28, 1197–1198.

Yu, L., Liu, Z., He, W., Chen, H. F., Lai, Z. L., Duan, Y. H., et al. (2020). Hydroxysafflor Yellow A confers neuroprotection from focal cerebral ischemia by modulating the crosstalk between JAK2/STAT3 and SOCS3 signaling pathways [published online ahead of print, 2020 Feb 14]. *Cell. Mol. Neurobiol.* 40 (8), 1271–1281. doi:10.1007/s10571-020-00812-7

Zang, B. X., Jin, M., Si, N., Zhang, Y., Wu, W., and Piao, Y. Z. (2002). Antagonistic effect of hydroxysafflor yellow A on the platelet activating factor receptor. *Yao Xue Xue Bao* 37, 696–699.

Zeng, Q. Y., Huang, X., Wang, Y., Lv, H. Y., Xia, Z., and Ji, H. (2013). Simultaneous determination of three metabolism constituents of Danchuanhong formula in urinein of patients with traumatic brain injury after oral administration by UPLC-ESI-MS/MS. *Pharmacol. Clin. Chin Materia. Med.* 29, 182–185.

Zhang, L., Zhu, L., Wang, Y. F., Jiang, Z. Z., Chai, X., Zhu, Y., et al. (2012). Characterization and quantification of major constituents of Xue Fu Zhu Yu by UPLC-DAD–MS/MS. *J. Pharmaceut. Biomed.* 62, 203–209. doi:10.1016/j.jpba.2011.12.026

Zhang, N., Xing, M. Y., Wang, Y. Y., Liang, H., Yang, Z., Shi, F. D., et al. (2014). Hydroxysafflor yellow A improves learning and memory in a rat model of vascular dementia by increasing VEGF and NR1 in the hippocampus. *Neurosci. Bull.* 30, 417–424. doi:10.1007/s12264-013-1375-2

Zhang, J., Li, J., Song, H., Xiong, Y., Liu, D., and Bai, X. (2019). Hydroxysafflor yellow A suppresses angiogenesis of hepatocellular carcinoma through inhibition of p38 MAPK phosphorylation. *Biomed. Pharmacother.* 109, 806–814. doi:10.1016/j.biopha.2018.09.086

Zhang, H. F. (2006). *Study on absorption mechanism of hydroxysafflor yellow A in gastrointestinal tract*. Beijing, China: Chin Pharmaceutical University.

Zhang, L. L., Tian, K., Tang, Z. H., Chen, X. J., Bian, Z. X., Wang, Y. T., et al. (2016). Phytochemistry and pharmacology of *Carthamus tinctorius* L. *Am. J. Chin. Med.* 44, 197–226. doi:10.1142/S0192415X16500130

Zhang, Y. D., Song, L. J., Pan, R. Y., Gao, J. W., Zang, B. X., and Jin, M. (2017). Hydroxysafflor yellow A alleviates lipopolysaccharide-induced acute respiratory distress syndrome in mice. *Biol. Pharm. Bull.* 40, 135–144. doi:10.1248/bpb.b16-00329

Zhang, Z., Guo, M., and Zhang, J. (2009). Identification of AFLP fragments linked to hydroxysafflor yellow A in *Flos Carthami* and conversion to a SCAR marker for rapid selection. *Mol. Breed.* 23, 229–237. doi:10.1007/s11032-008-9228-9

Zhao, B., Gu, S., Du, Y., Shen, M., Liu, X., and Shen, Y. (2018). Solid lipid nanoparticles as carriers for oral delivery of hydroxysafflor yellow A. *Int. J. Pharm. (Amst.)* 535, 164–171. doi:10.1016/j.ijpharm.2017.10.040

Zhao, X. P. (2015). *The evaluation and breeding selection of Safflower germplasm resources*. Henan, China: Henan Normal University.

Zheng, M., Guo, X. J., Pan, R. Y., Gao, J. W., Zang, B. X., and Jin, M. (2019). Hydroxysafflor yellow A alleviates ovalbumin-induced asthma in a Guinea pig model by attenuateing the expression of inflammatory cytokines and signal transduction. *Front. Pharmacol.* 10, 328. doi:10.3389/fphar.2019.00328

Zhou, P., Zhou, H. F., He, Y., Zhang, Y. Y., Yang, J. H., Dai, L. L., et al. (2014). Transport characteristics of hydroxysafflor yellow A across Caco-2 cell monolayer model. *Chin. Tradit. Herb. Drugs* 45, 2030–2035. doi:10.7501/j.issn.0253-2670.2014.14.014

Zhou, J., Li, M., Jin, W., Li, X., Fan, H., and Zhang, Y. (2018). Pharmacokinetic study on protocatechuic aldehyde and hydroxysafflor yellow A of Danhong injection in rats with hyperlipidemia. *Pharmacology* 102, 154–160. doi:10.1159/000491020

Zhou, D. L., Ding, T. T., Ni, B., Jing, Y. Y., and Liu, S. X. (2019). Hydroxysafflor Yellow A mitigated myocardial ischemia/reperfusion injury by inhibiting the activation of the JAK2/STAT1 pathway. *Int. J. Mol. Med.* 44, 405–416. doi:10.3892/ijmm.2019.4230

Zhu, H. J., Wang, L. J., Wang, X. Q., Pan, H., Li, N. S., Yang, H. B., et al. (2015). Hydroxysafflor yellow A (HYSA) inhibited the proliferation and differentiation of 3T3-L1 preadipocytes. *Cytotechnology* 67, 885–892. doi:10.1007/s10616-014-9783-3

Zhu, M.-Z., Zhou, Z.-Y., Zhou, Z.-Y., Lu, H., Gao, M., Liu, L.-M., et al. (2020). Effect and safety of hydroxysafflor yellow a for injection in patients with acute ischemic stroke of blood stasis syndrome: a phase II, multicenter, randomized, double-blind, multiple-dose, active-controlled clinical trial. *Chin. J. Integr. Med.* 26, 420–427. doi:10.1007/s11655-020-3094-7

Zong, X., Li, L., Zhang, H., Li, B., and Liu, C. (2013). Preparative separation of hydroxyl safflower yellow A and anhydrosafflor yellow B in plant extract of *Carthamus Tinctorius* L. by reverse-phase medium-pressure liquid chromatography. *J. Liq. Chromatogr. Relat. Technol.* 36. doi:10.1080/10826076.2012.704614

Zou, J., Wang, N., Liu, M., Bai, Y., Wang, H., Liu, K., et al. (2018). Nucleolin mediated pro-angiogenic role of Hydroxysafflor Yellow A in ischaemic cardiac dysfunction: Post-transcriptional regulation of VEGF-A and MMP-9. *J. Cell. Mol. Med.* 22. 2692–2705. doi:10.1080/10826076.2012.704614

Conflict of Interest: The authors declare that the research was conducted in the absence of any commercial or financial relationships that could be construed as a potential conflict of interest.

The handling Editor declared a past co-authorship with one of the authors HX.

GLOSSARY

AUMC the plasma concentration-time curve
BBB the blood-brain barrier
DAD diode
DDAB dimethyl octadecyl ammonium bromide
ECD electrochemical
EDTA ethylenediaminetetraacetic acid
HIF-1 α hypoxia-inducible factor-1 α
HO-1 hemeoxygenase-1
HSYA Hydroxysafflor yellow A
I/R ischemia/reperfusion
LAD left anterior descending coronary artery
LOD the limits of detection
LOQ the limit of quantification
MCAO middle cerebral artery occlusion
MIS myocardial infarction size
Nrf2 nuclear factor erythroid 2-related factor 2
MSPD Matrix solid-phase dispersion
OGD oxygen and glucose deprivation models
PAH pulmonary arterial hypertension
Papp the apparent permeability coefficient
P-gp P-glycoprotein
SDEDDS Self-emulsifying drug delivery system
SLN Solid lipid nanoparticles
SY safflower yellow
TBI traumatic brain injury
UAE ultrasound-assisted treatment.